Lecture 8: Geometric Modeling and Visualization

Finite Elements from Imaging I & II:
Active Contouring, Segmentation, Reconstruction

Chandrajit Bajaj

Center for Computational Visualization
Institute of Computational and Engineering Sciences
Department of Computer Sciences
University of Texas at Austin

November 2007

The Context: Structure Determination via Cryo-EM

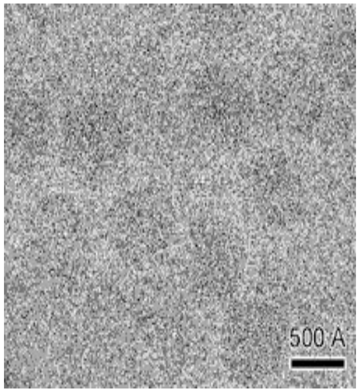

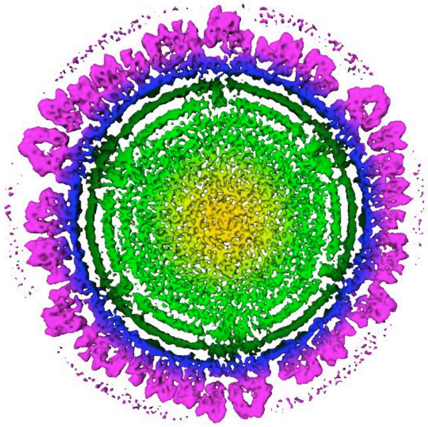

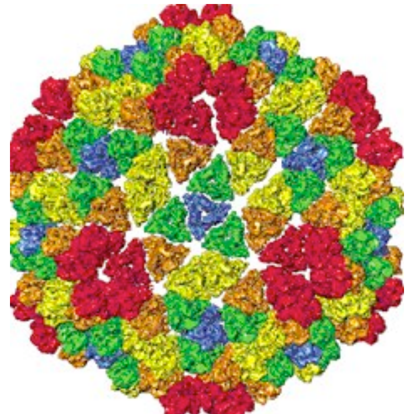

h=3, k=1, T=13

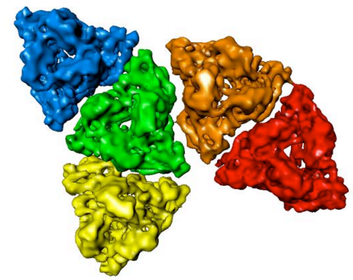

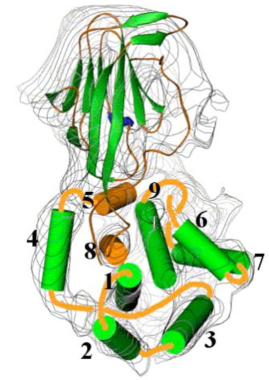

→ Cryo-EM images

→ Reconstructed density maps

→ Structure Segmentation

→ Sub-Atomic Modeling

→ Functional Analysis

→ Visualization

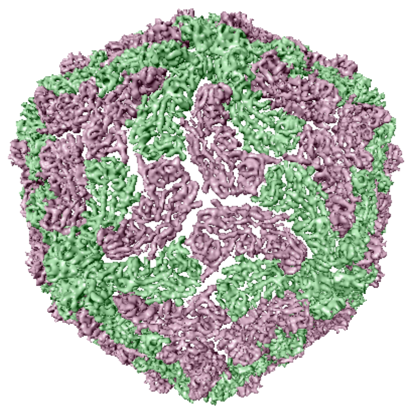

h=1, k=0, T=1

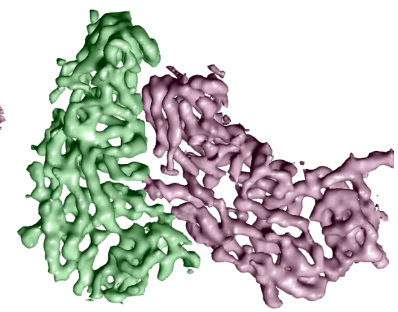

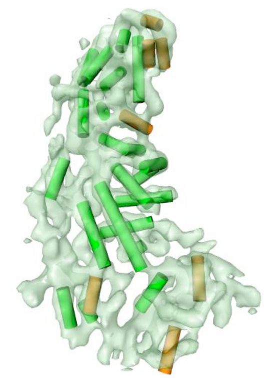

- Collaborators:
  Dr. Wah Chiu, NCMI,BCM(Houston);
  Dr. Andrej Sali, UCSF
- Sponsored by NSF-ITR

Problem Description

Rice Dwarf Virus

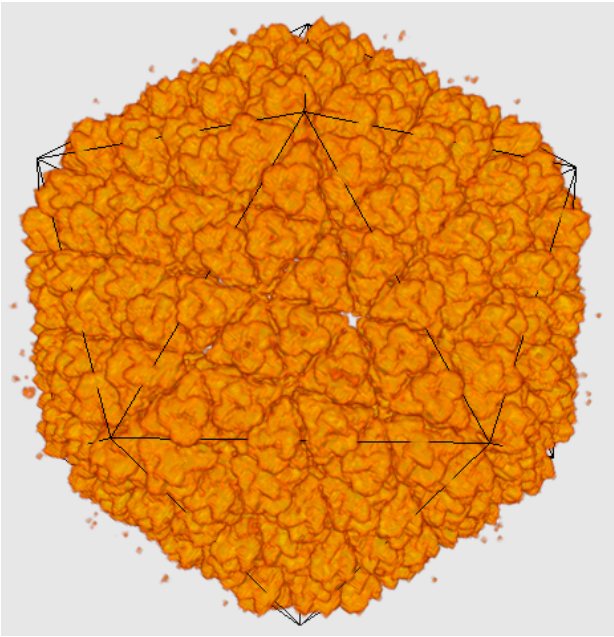

segmented outer capsid layer with icosahedral symmetry

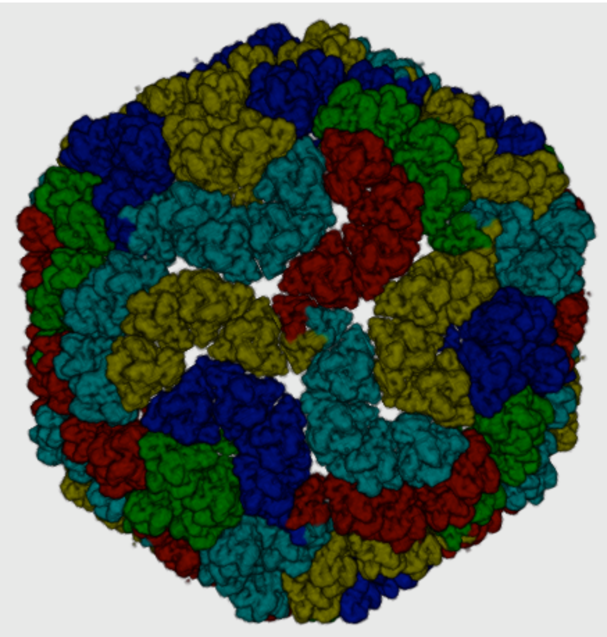

segmented asymmetric subunits

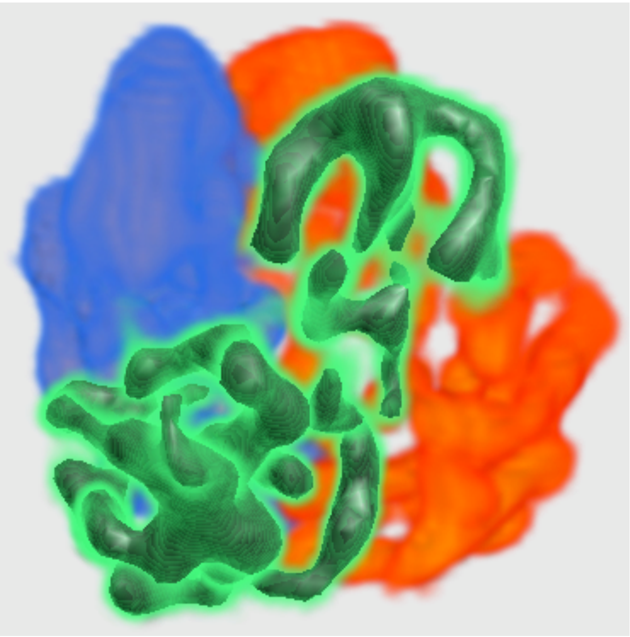

segmented monomer (protein)

Algorithm Overview

- Three steps:
  - Detection of critical points
    (Anisotropic vector diffusion)
  - Detection of icosahedral symmetry
    (Five-fold symmetry detection)
  - Segmentation of asymmetric subunits
    (A variant of the fast marching method)

Detecting Critical Points

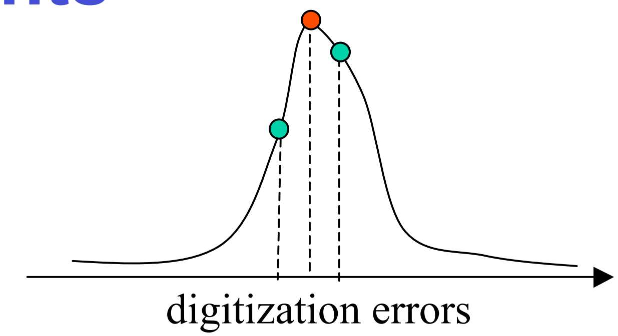

- Three types
  - – maximal, minimal, saddle

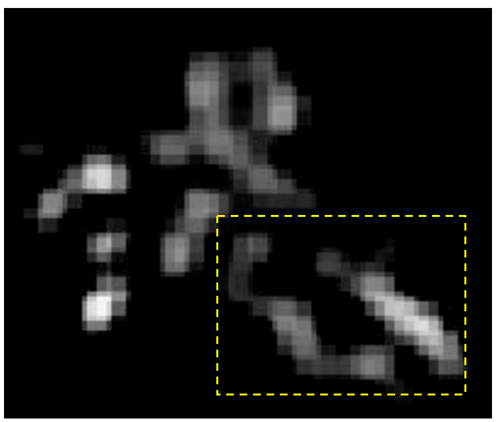

density map

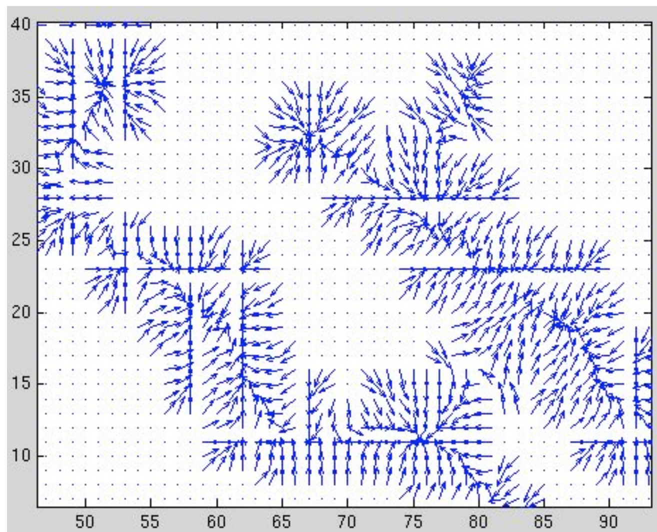

initial gradient vector field

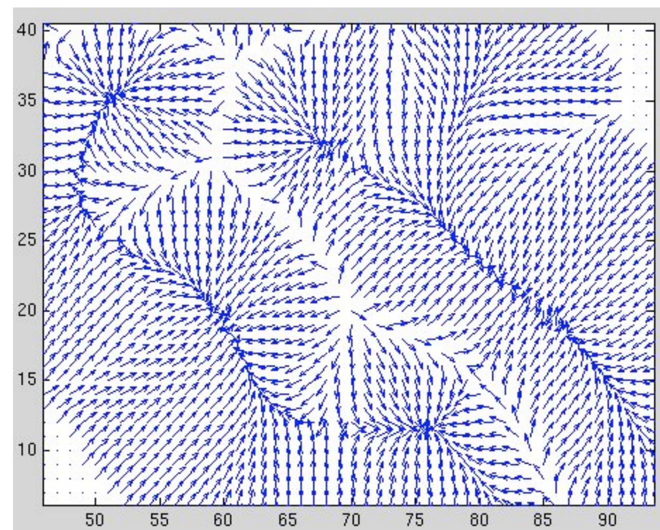

diffused vector field

Detecting Critical Points (contd.)

- Gradient vector diffusion:
  - smoothing the vector fields
  - diffusion to the flat regions

Isotropic diffusion

$$\begin{cases} \dfrac{\partial u}{\partial t} = \mu \cdot \nabla^2 u \\ \dfrac{\partial v}{\partial t} = \mu \cdot \nabla^2 v \end{cases}$$

where

(u, v) are gradient vector.

Anisotropic diffusion

$$\begin{cases} \dfrac{\partial u}{\partial t} = \mu \cdot div(g(\alpha)\nabla u) \\ \dfrac{\partial v}{\partial t} = \mu \cdot div(g(\alpha)\nabla v) \end{cases}$$

where $g(\alpha)$ is a decreasing function

α is the angle between the central pixel and its surrounding pixels.

Detecting Critical Points (contd.)

- Sink points $\Leftrightarrow$ maximal critical points

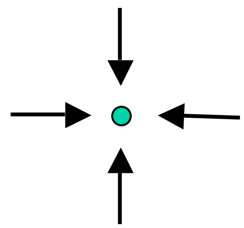

- Source points $\Leftrightarrow$ minimal critical points

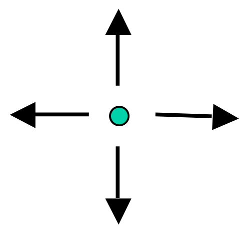

- Sink&source points $\Leftrightarrow$ saddle critical points

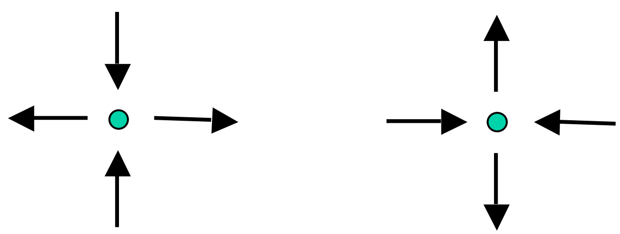

Detecting Critical Points (contd.)

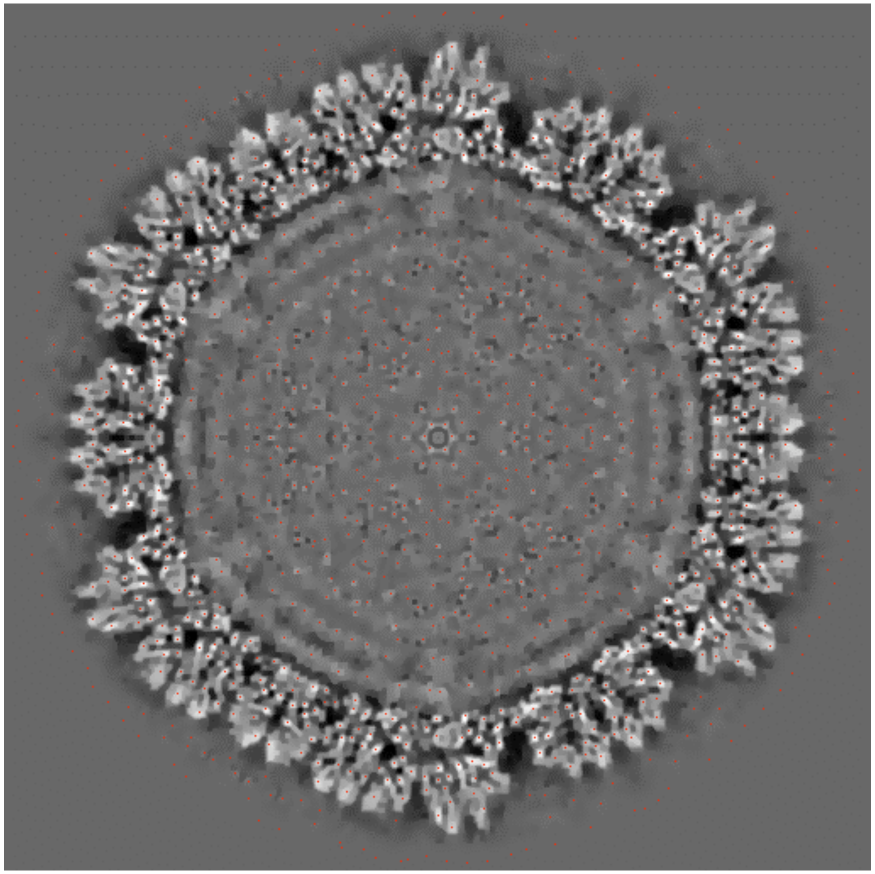

- We consider only the maximal critical points
- Used for two purposes:
  - Speed up the symmetry detection
  - Seed points in the fast marching method

Symmetry Detection

- Icosahedral symmetry overview (Caspar & Klug 1962; Baker et al. 1999)

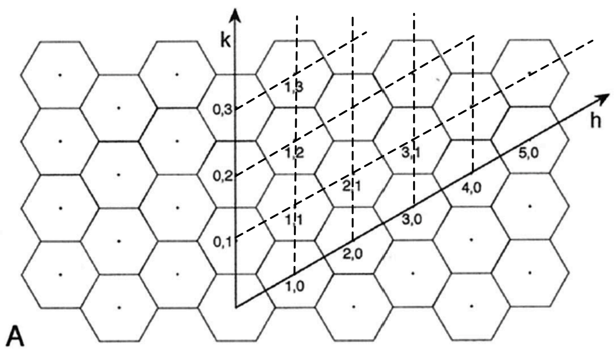

h k	T	Example
1 0	1	bacteriophage φX174
1 1	3	tomato bushy stunt virus
2 0	4	Sindbis virus
1 2	7*d*	polyoma virus
3 1	13*l*	reovirus
1 3	13*d*	infectious bursal disease virus
4 0	16	herpesvirus
5 0	25	adenovirus

Notations: *d* = *dextro* (right handed)

l = *laevo* (left handed)

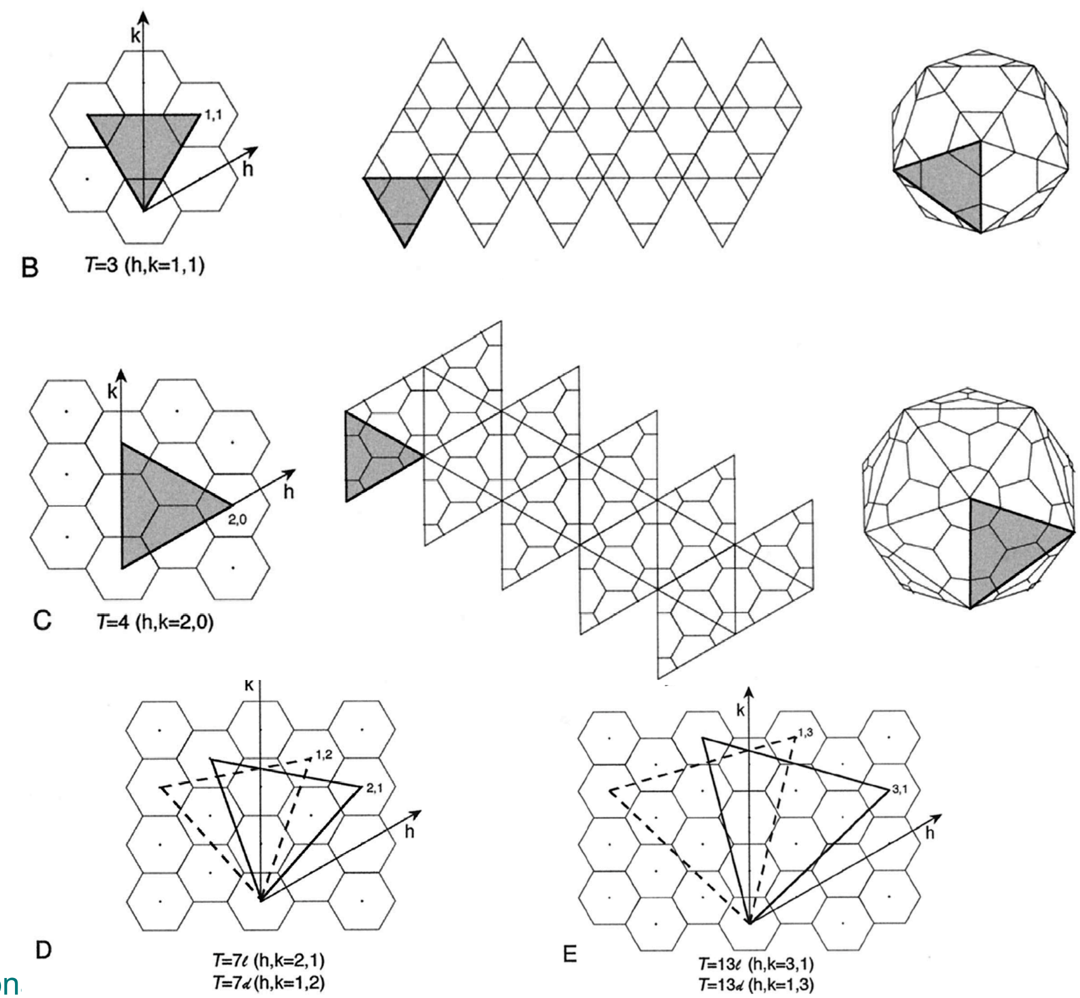

Symmetry Detection (contd.)

- Asymmetric subunits in an icosahedra

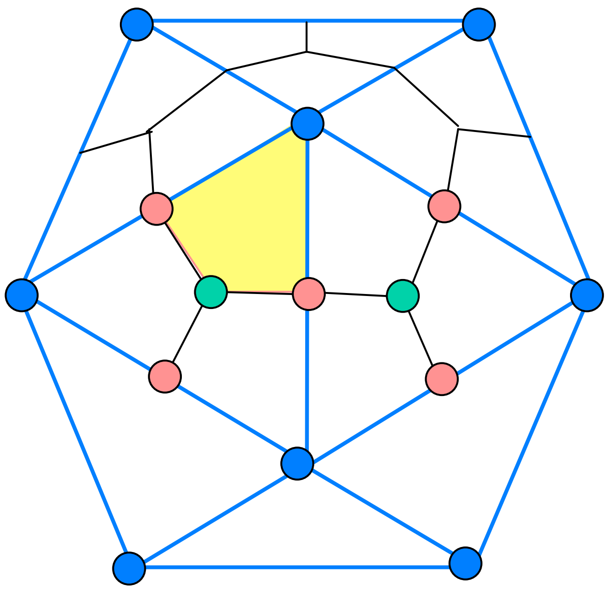

Two-fold vertices

Three-fold vertices

Five-fold vertices

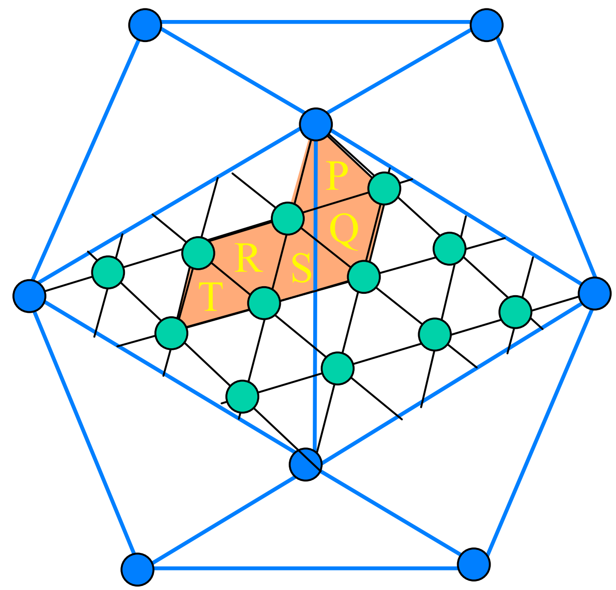

Example: RDV

Task: detect all 12 five-fold symmetry axes !

Symmetry Detection (contd.)

- Detect five-fold symmetry axes

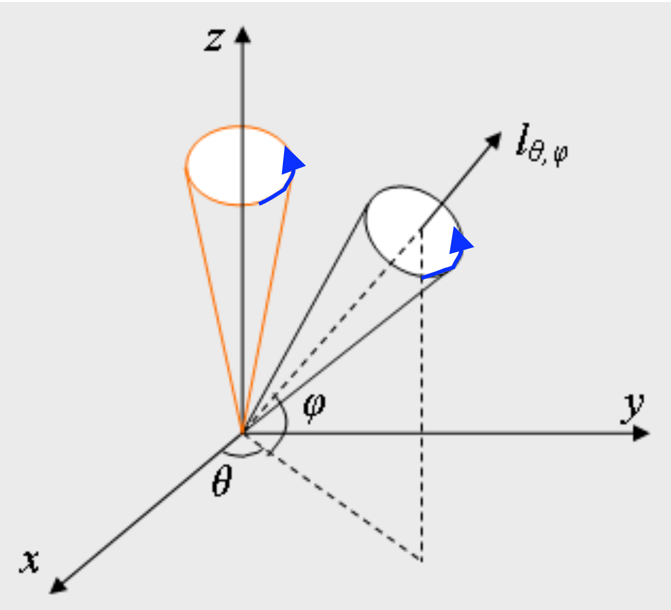

$$f(\vec{r}) = f(R_{(\theta,\varphi,2\pi/5)} \cdot \vec{r}) \quad \text{for } \forall \vec{r}$$

$R_{(\theta,\varphi,\alpha)}$ is the rotation around $l_{\theta,\varphi}$ by a amount of α

$$R_{(\theta,\varphi,\alpha)} = A^{-1} \cdot B^{-1} \cdot \begin{pmatrix} \cos(\alpha) & -\sin(\alpha) & 0 \\ \sin(\alpha) & \cos(\alpha) & 0 \\ 0 & 0 & 1 \end{pmatrix} \cdot B \cdot A$$

Symmetry Detection (contd.)

- Detect five-fold symmetry axes

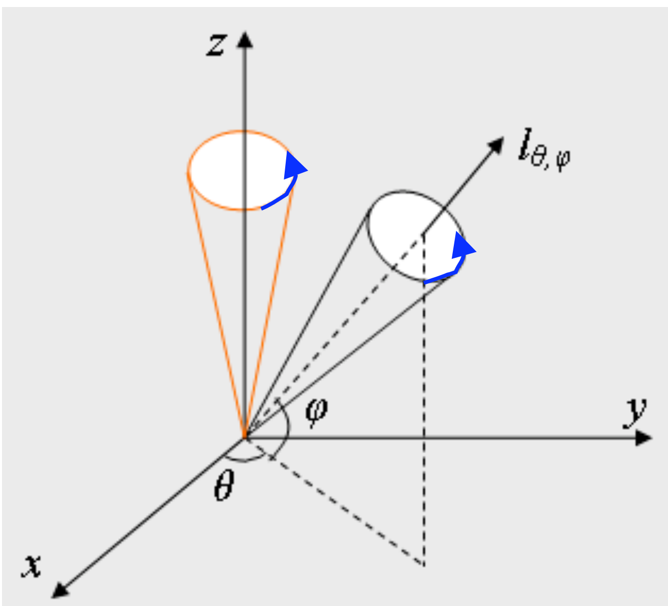

$$R_{(\theta,\varphi,\alpha)} = A^{-1}\cdot B^{-1}\cdot\begin{pmatrix}\cos(\alpha) & -\sin(\alpha) & 0\\ \sin(\alpha) & \cos(\alpha) & 0\\ 0 & 0 & 1\end{pmatrix}\cdot B\cdot A$$

$$A = \begin{pmatrix}\cos(\theta) & \sin(\theta) & 0\\ -\sin(\theta) & \cos(\theta) & 0\\ 0 & 0 & 1\end{pmatrix}$$

$$B = \begin{pmatrix}\cos(\frac{\pi}{2}-\varphi) & 0 & -\sin(\frac{\pi}{2}-\varphi)\\ 0 & 1 & 0\\ \sin(\frac{\pi}{2}-\varphi) & 0 & \cos(\frac{\pi}{2}-\varphi)\end{pmatrix}$$

Symmetry Detection (contd.)

- Direct correlation

$$C(\theta,\varphi)=\sum_{\vec{r}\in V} f(\vec{r})f(R_{(\theta,\varphi,2\pi/5)}\cdot\vec{r})$$

Total time: $O(MN)$

M: total number of angular bins

N: total number of voxels (e.g., 512^3)

- Solutions: reduce M
  - Principal axis evaluation
  - Hierarchical sampling
- One solution: reduce N

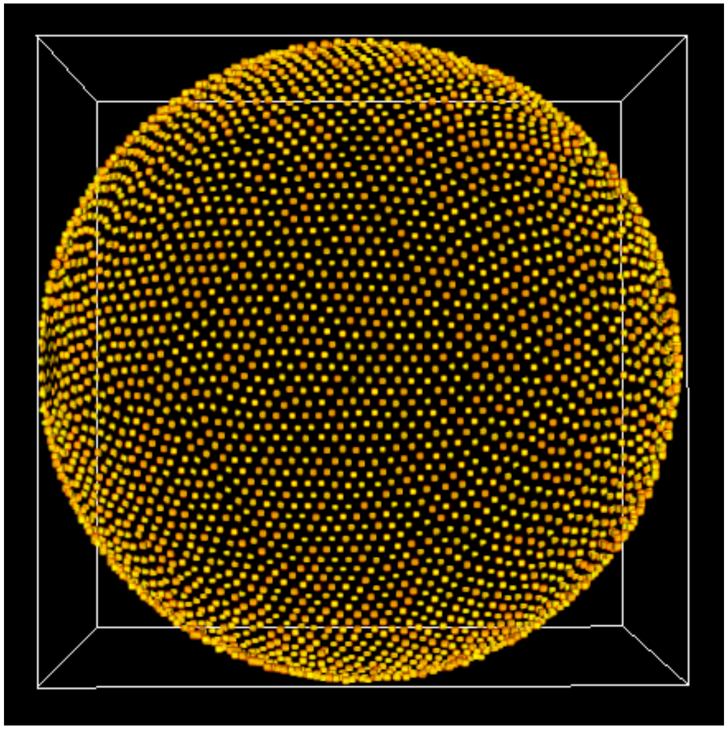

~ 46,000 angular bins

Symmetry Detection (contd.)

- Algorithm: *detect 5-fold rotation symmetry*
  - Compute the scoring function
    - For every angular bin B_j, compute θ_j, φ_j {

      For every critical points C_i {

$$\vec{r}_k(C_i, B_j) = R_{(\theta_j, \varphi_j, 2k\pi/5)} \cdot C_i, \quad k = 0,1,2,3,4$$

$$Dev(C_i, B_j) = \frac{1}{5}\sum_{k=0}^{4}(f(\vec{r}_k) - \bar{f}) \ \}$$

$$SF(B_j) = \frac{1}{p}\sum_{i=0}^{p} Dev(C_i, B_j) \ \}$$

  - Locate the symmetry axes
    - The 12 peaks
  - Refine the symmetry axes
    - In order to generate a perfect icosahedra (rotate the axes by 0^0, 63.43^0, 116.57^0, 180^0)

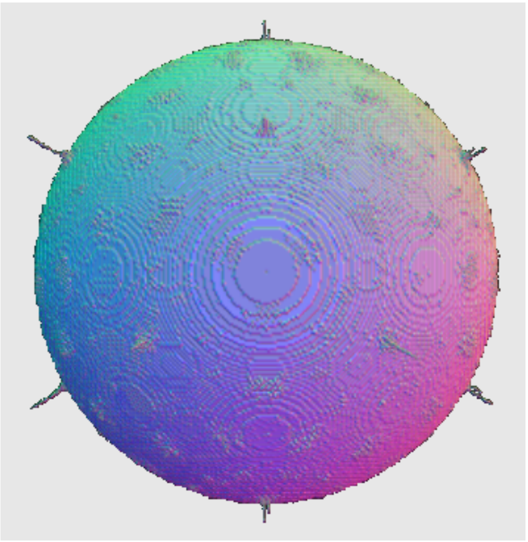

Inverted and normalized SF(Bj)

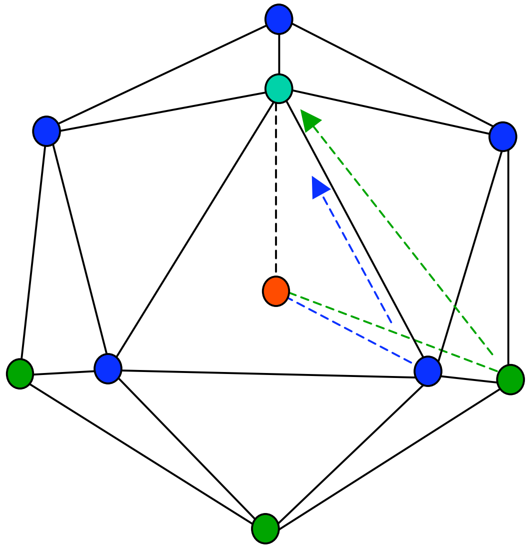

Symmetry Detection (contd.)

- Performance evaluation: *RDV outer layer*

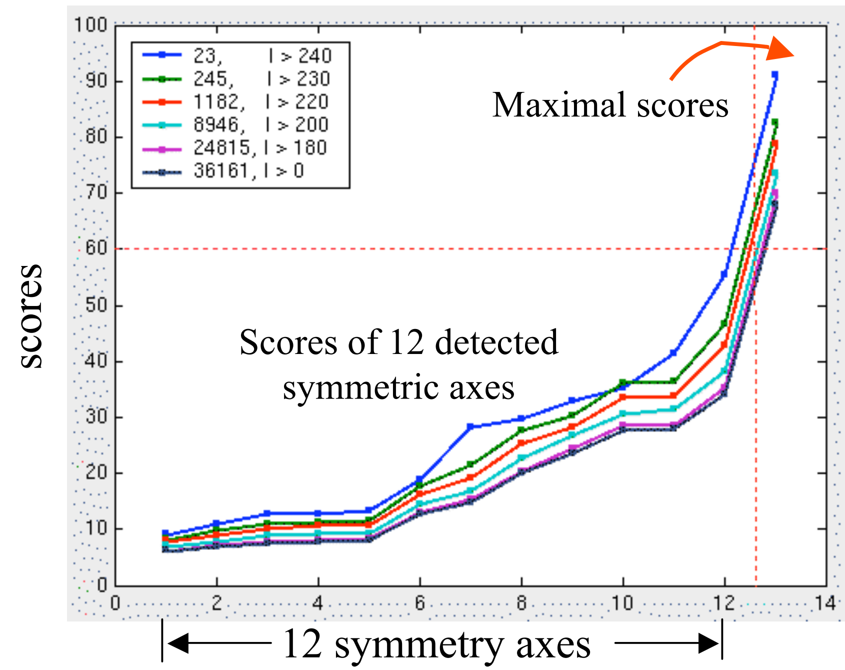

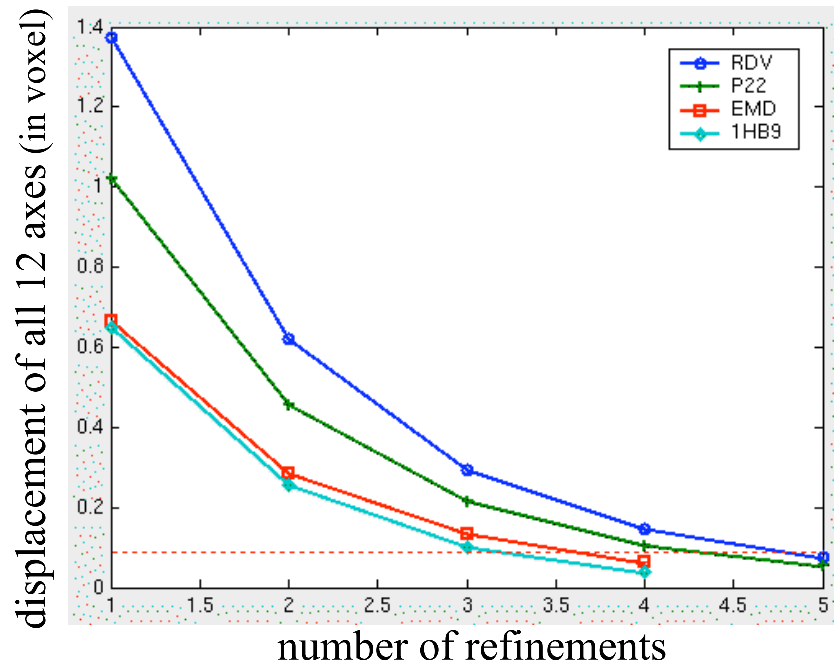

$O(MN)$ M: 46,012

N: $512^3 \rightarrow 36{,}161 \rightarrow 23$

Test on number of refinements

Asymmetric Subunit Segmentation

- A simple case

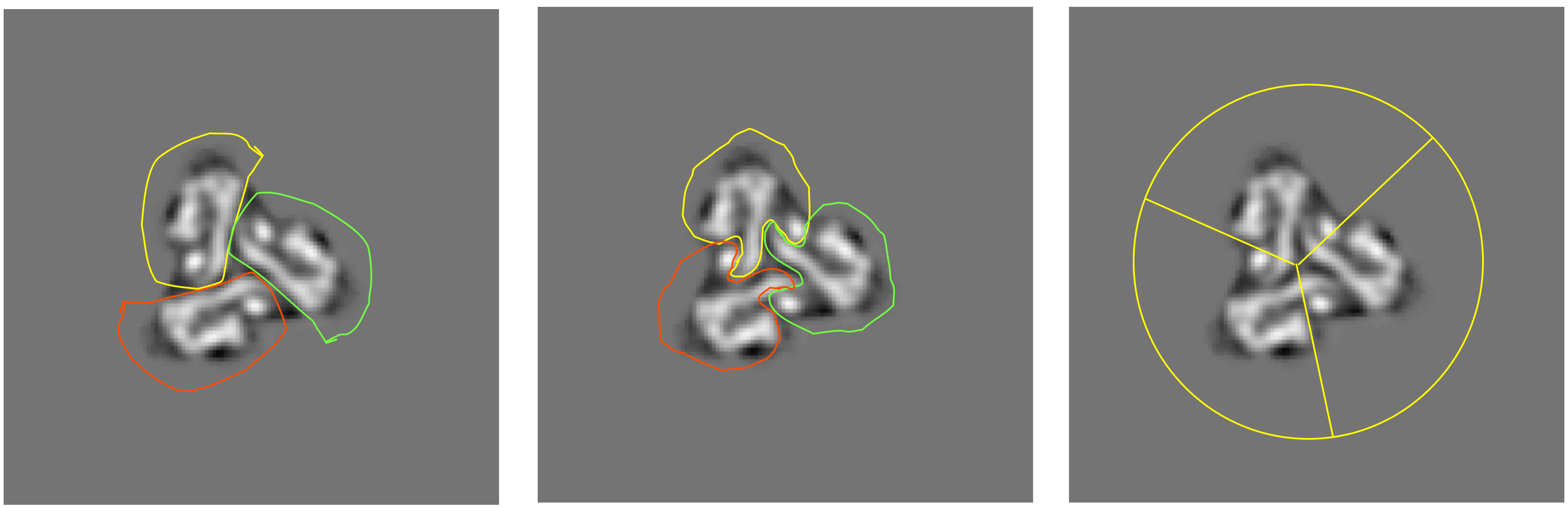

Infinite number of partitionings

which one is the best?

Asymmetric Subunit Segmentation (contd.)

- The criterion for partitioning a symmetric image

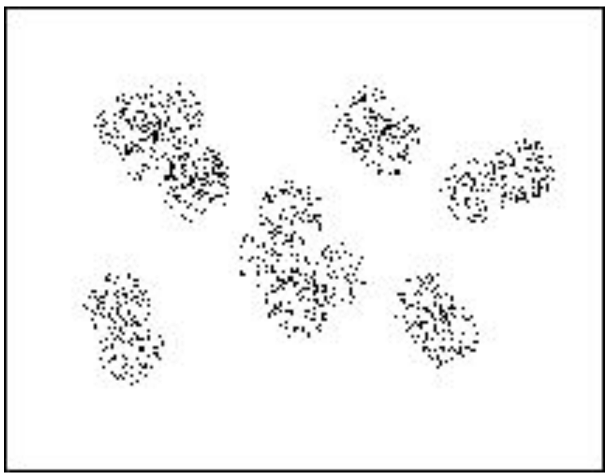

A related problem: data clustering

Criterion: distance !

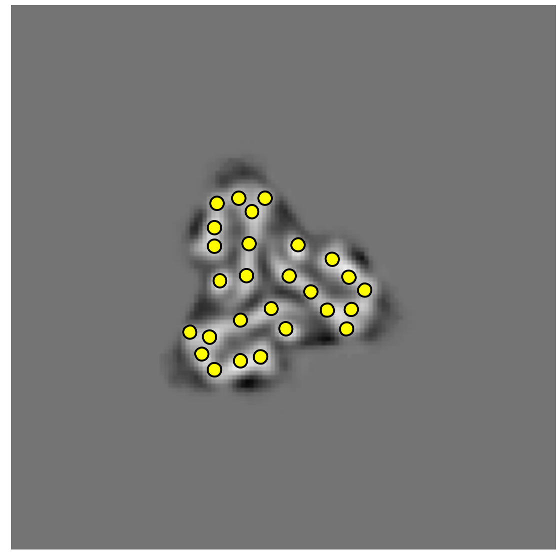

Classifying critical points

Task: distance !

Asymmetric Subunit Segmentation (contd.)

- Marching distance

$$MD_f(A,B) = Min\{ \int_{A \to B} e^{\|\nabla f(\vec{r})\|} ds \}$$ along all paths from A to B

$$MD_f(A,B) = Min\{ \sum_{\vec{r}=A}^{B} e^{\|\nabla f(\vec{r})\|} - \frac{e^{\|\nabla f(A)\|} + e^{\|\nabla f(B)\|}}{2} \}$$ (discrete form)

Closely related to the fast marching method !

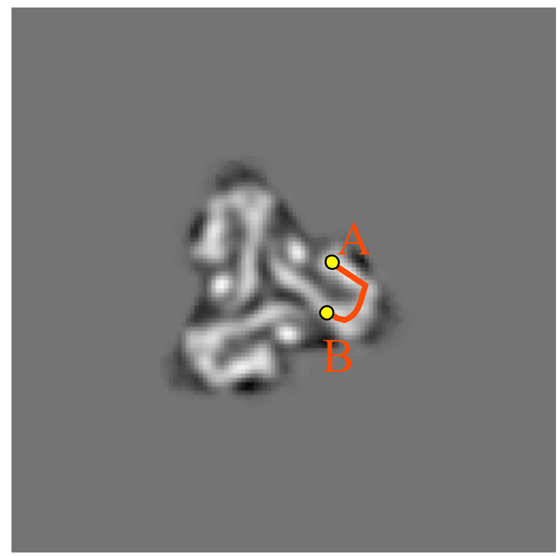

Asymmetric Subunit Segmentation (contd.)

- The fast marching method

  Start from a seed and propagate by certain speed

$$\left\|\nabla T(\vec{r})\right\| \cdot F(\vec{r}) = 1$$

where F is the speed function, which can be defined as:

$$F(\vec{r}) = e^{-\alpha\left\|\nabla F(\vec{r})\right\|} \qquad \alpha > 0$$

The map T gives the *marching distances* from the seed to all the other points

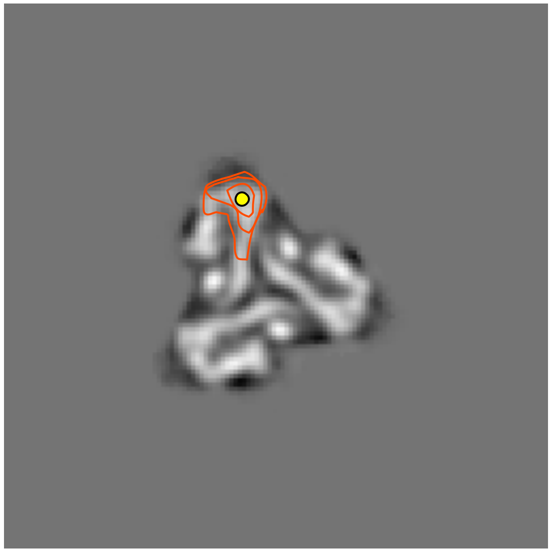

Asymmetric Subunit Segmentation (contd.)

- The multi-seeded fast marching method

  Start from seeds and propagate independently by:

$$\left\|\nabla T(\vec{r})\right\| \cdot F(\vec{r}) = 1$$

where F is the speed function, which can be defined as:

$$F(\vec{r}) = e^{-\alpha\left\|\nabla F(\vec{r})\right\|} \qquad \alpha > 0$$

The map T gives the *marching distances* from the seed to all the other points

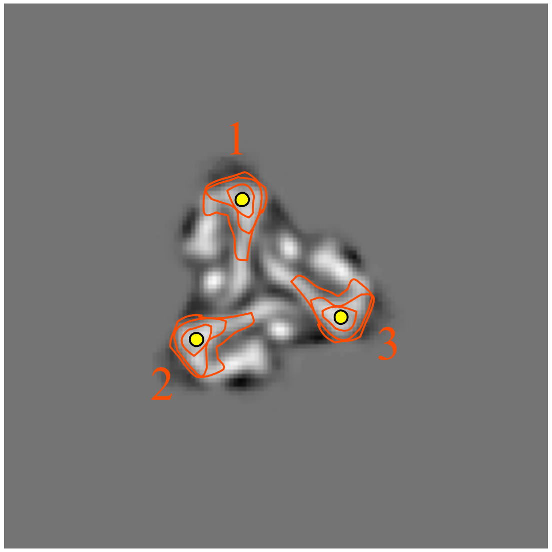

problem

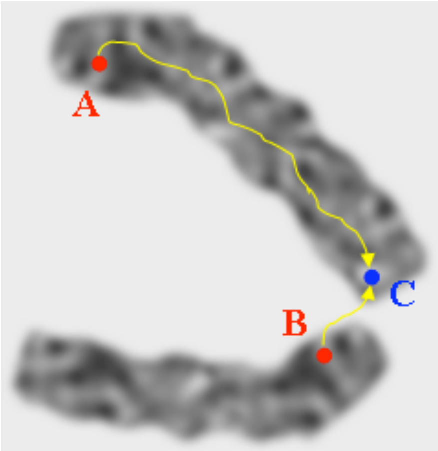

Asymmetric Subunit Segmentation (contd.)

- The solution
  - Use multiple seed points for each subunit
- The overall algorithm
  - Detect the critical points
  - Classify the critical points
  - Use the multi-seeded fast marching method
    - Merge for contours of the same group
    - Stop for contours of different groups

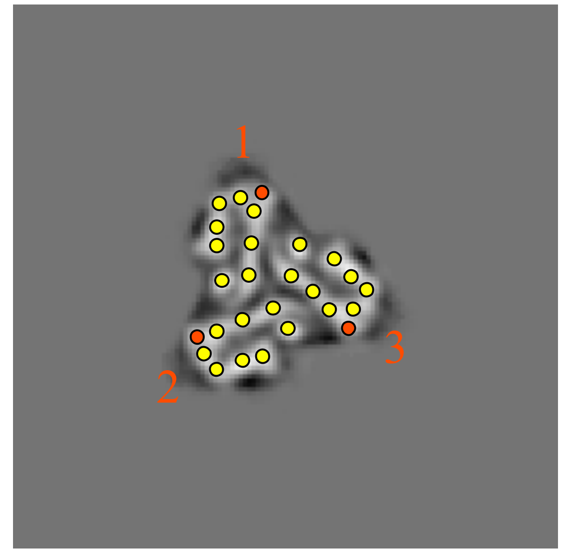

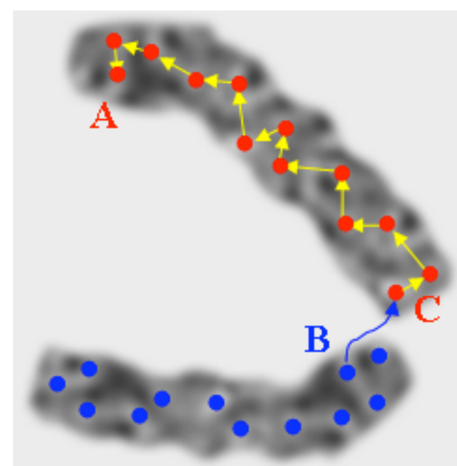

Asymmetric Subunit Segmentation (contd.)

- Segmentation of capsid layers

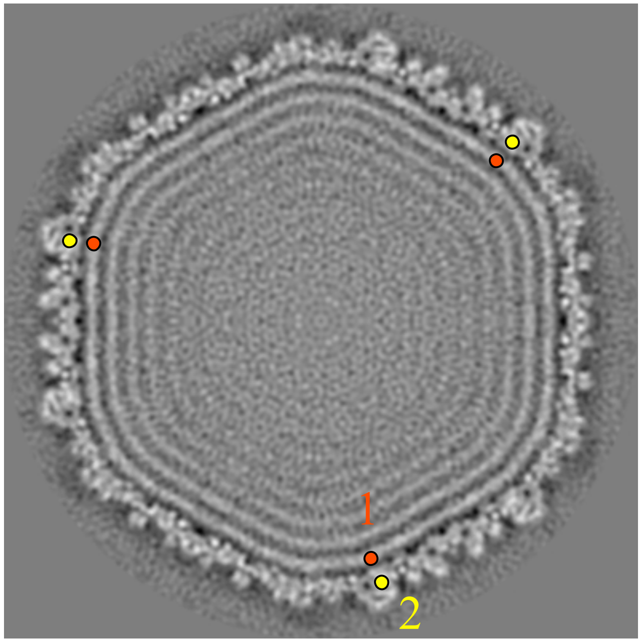

selection of seeds (manually)

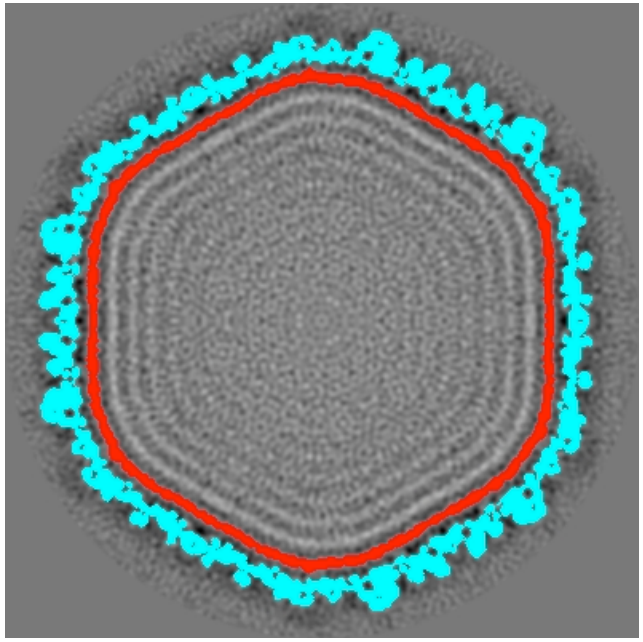

segmented capsid layer

Bacteriophage P22

Asymmetric Subunit Segmentation (contd.)

- Asymmetric subunit of icosahedral maps
  - 12 vertices, 60 subunits

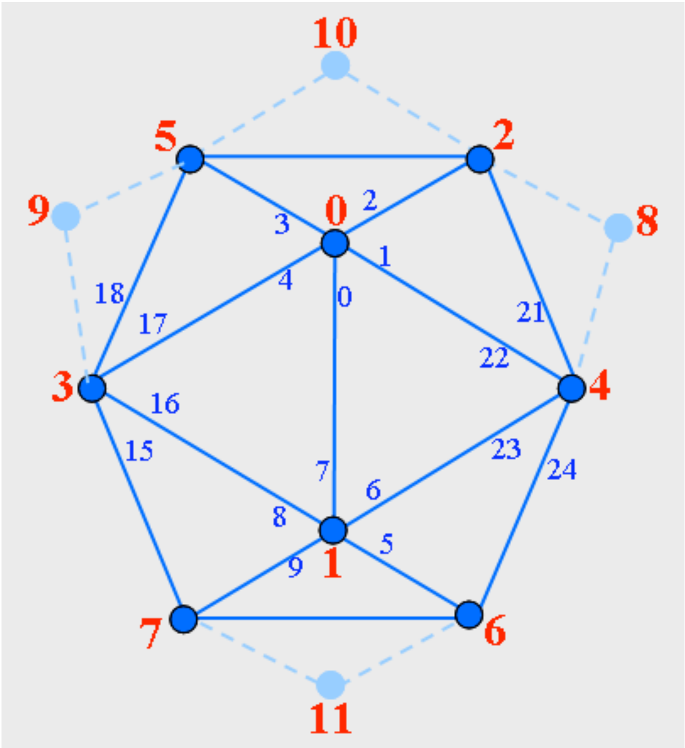

$$
\begin{cases}
index = 1; \\
for(i = 1; i < 5; i++)\{ \\
\quad Q = R^0_{2i\pi/5}(P); \\
\quad \text{assign } index \text{ to } Q; \\
\quad index++;\} \\
\\
for(j = 1; j < 11; j++)\{ \\
\quad P' = R_{0\to j}(P); \\
\quad for(i = 0; i < 5; i++)\{ \\
\quad\quad Q = R^j_{(2i+1)\pi/5}(P'); \\
\quad\quad \text{assign } index \text{ to } Q; \\
\quad\quad index++;\}\} \\
\\
P' = R_{0\to 11}(P); \\
for(i = 0; i < 5; i++)\{ \\
\quad Q = R^{11}_{2i\pi/5}(P'); \\
\quad \text{assign } index \text{ to } Q; \\
\quad index++;\}
\end{cases}
$$

Start from index 0

Asymmetric Subunit Segmentation (contd.)

- Asymmetric subunit of icosahedral maps
  - 12 vertices, 60 subunits

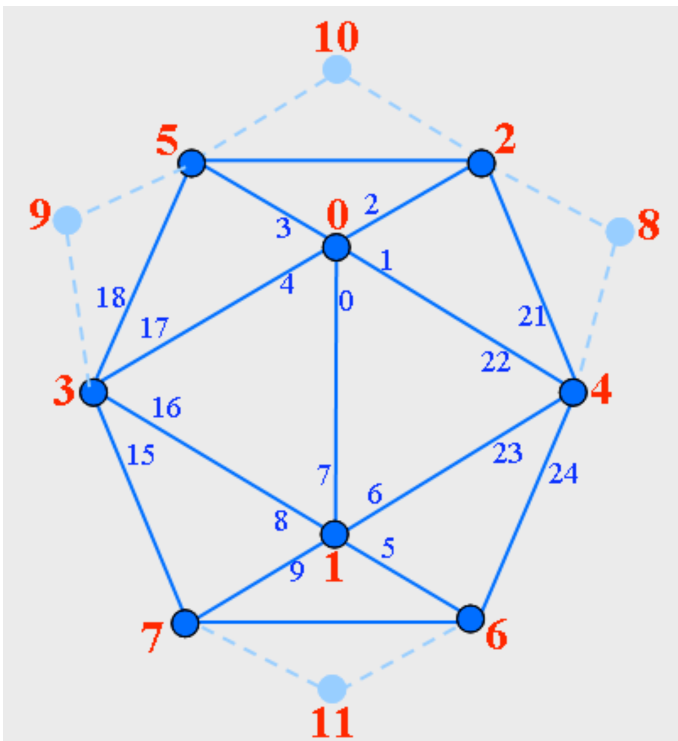

$$
\begin{cases}
if\,(j == 0) \\
\qquad B_0 = R^0{}_{-2i\pi/5}(B); \\
\\
else\,if\,(j < 11)\,\{ \\
\qquad B' = R^j{}_{-(2i+1)\pi/5}(B); \\
\qquad B_0 = R_{j\to 0}(B');\,\} \\
\\
else\,if\,(j == 11)\,\{ \\
\qquad B' = R^{11}{}_{-2i\pi/5}(B); \\
\qquad B_0 = R_{11\to 0}(B');\,\}
\end{cases}
$$

Start from any index

Results: Rice Dwarf Virus (6.8Å) (Zhou et al 2001)

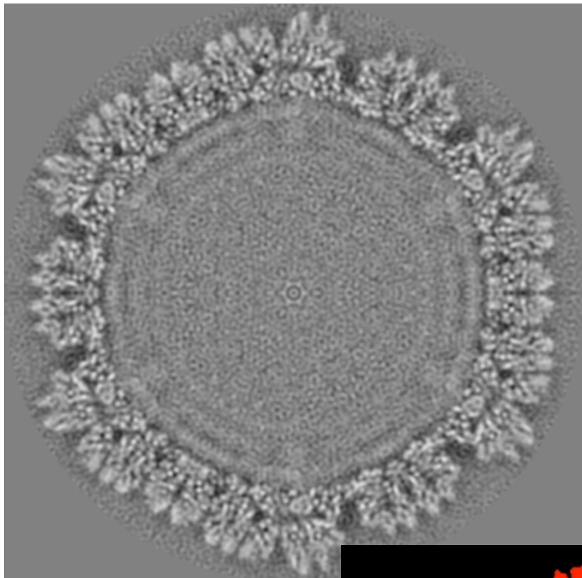

original map

(slice)

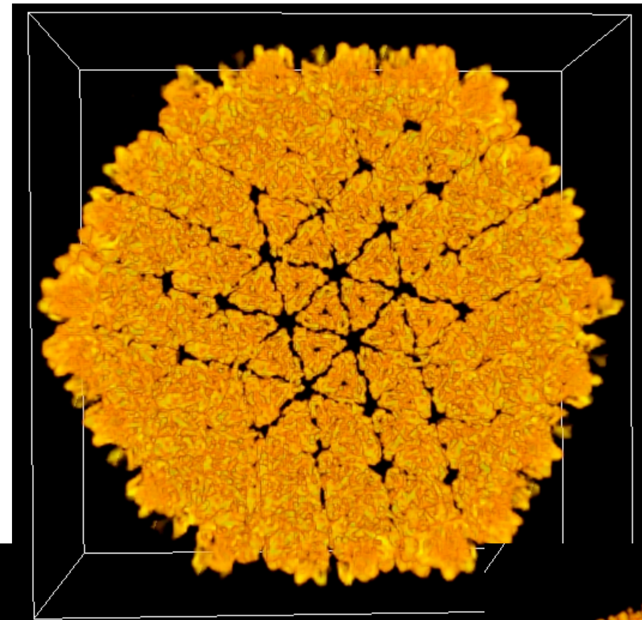

segmented outer layer

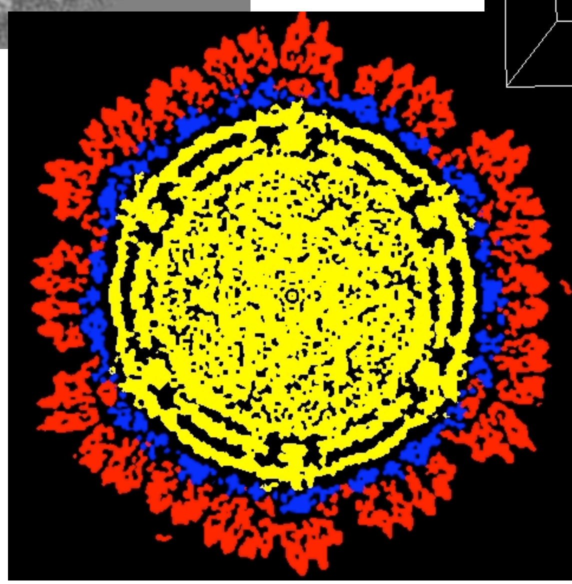

segmented map

(slice)

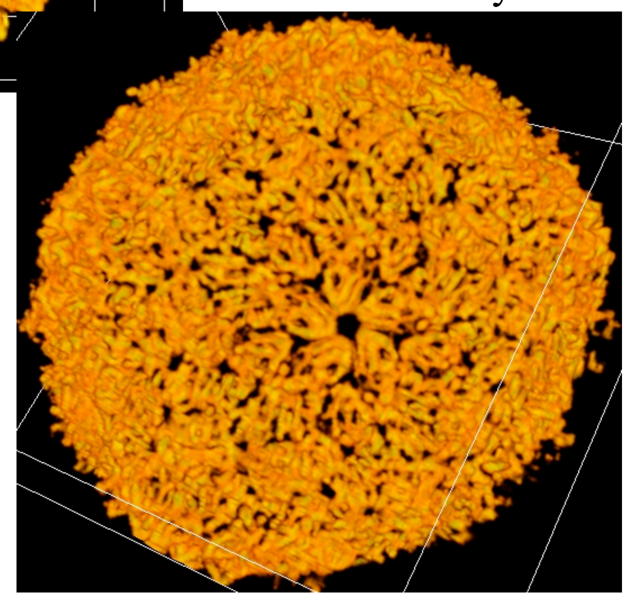

segmented inner layer

Results: Rice Dwarf Virus (6.8Å) (Zhou et al 2001)

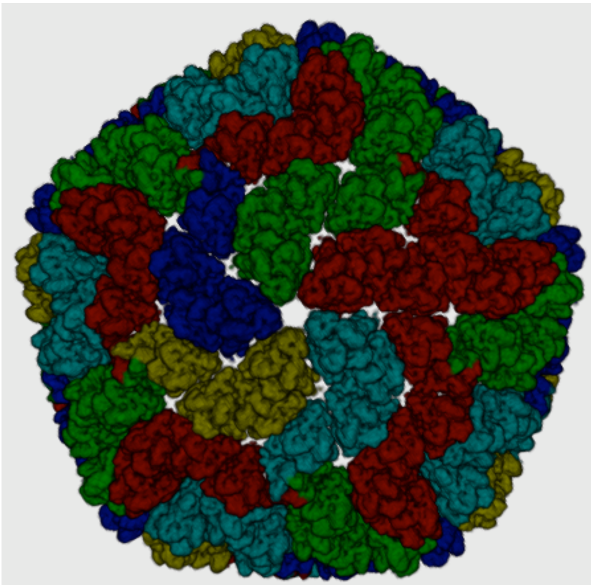

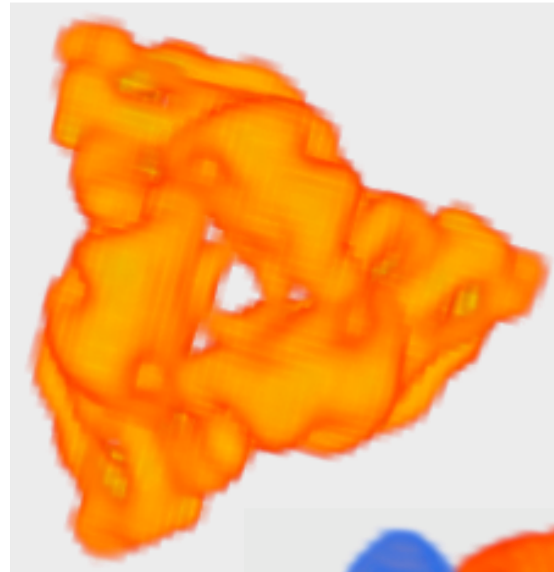

trimer &
segmented
mononer

asymmetric subunits of
outer layer

(five-fold & three-fold)

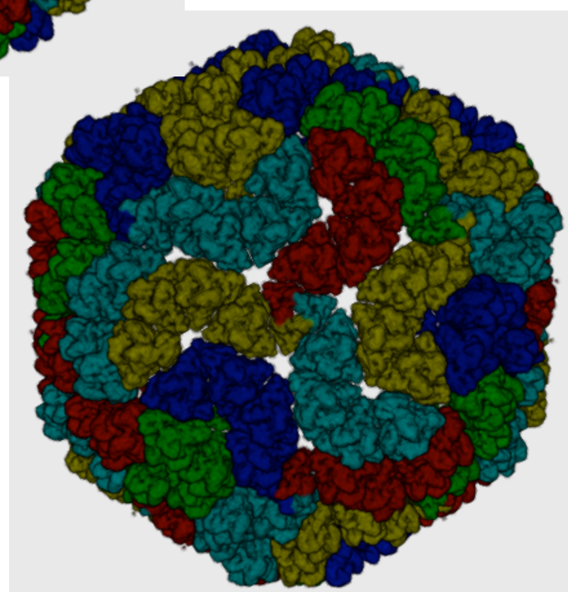

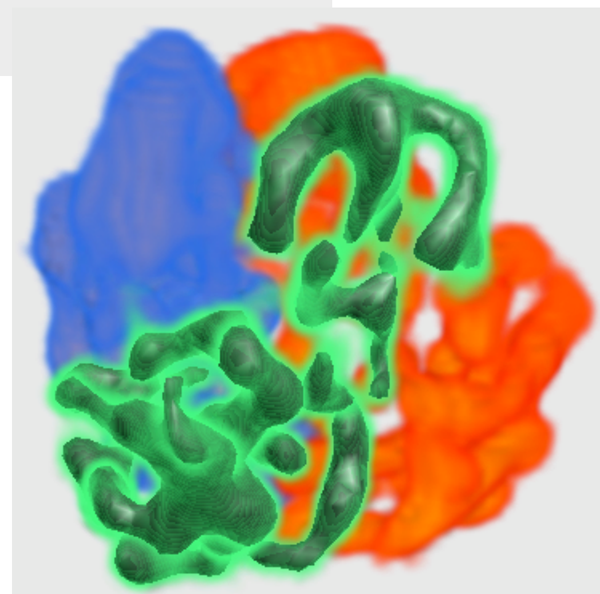

Results: Bacteriophage P22 (9.5Å)
(Jiang et al 2003)

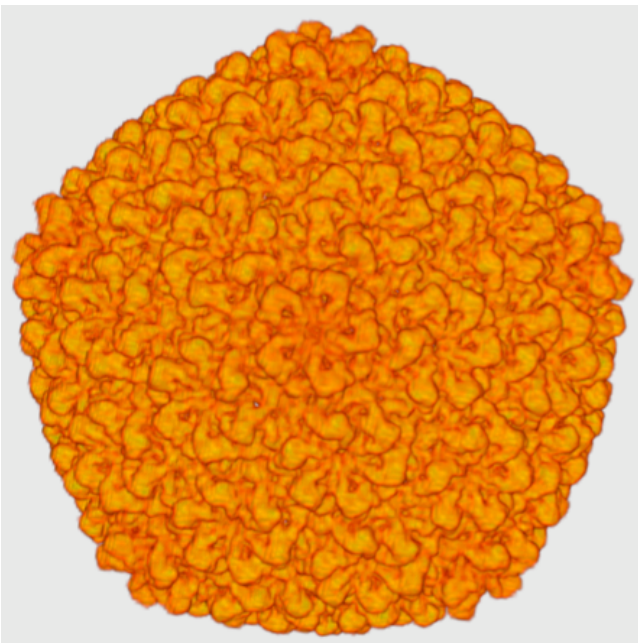
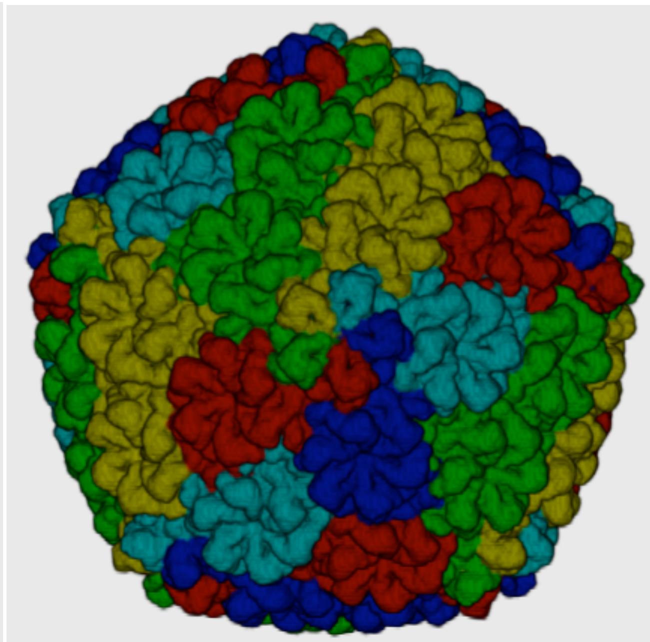
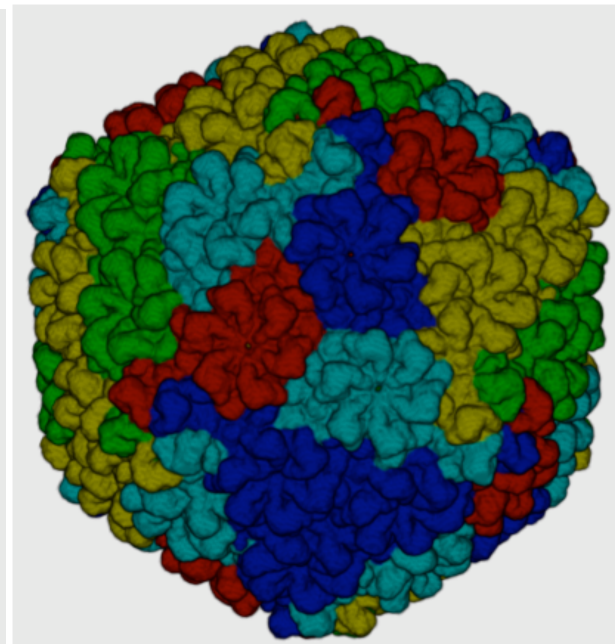

segmented capsid layer

segmented asymmetric subunits (five-fold & three-fold)

Results: Semliki Forest Virus (9.0Å)
(Mancini et al 2000)

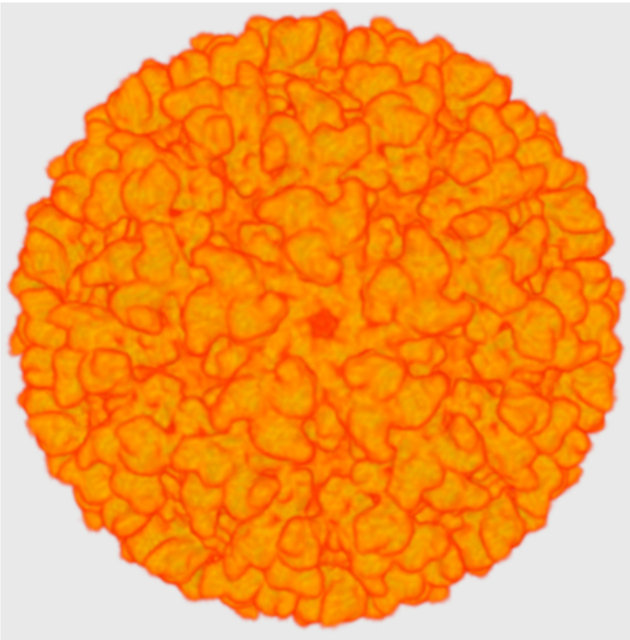

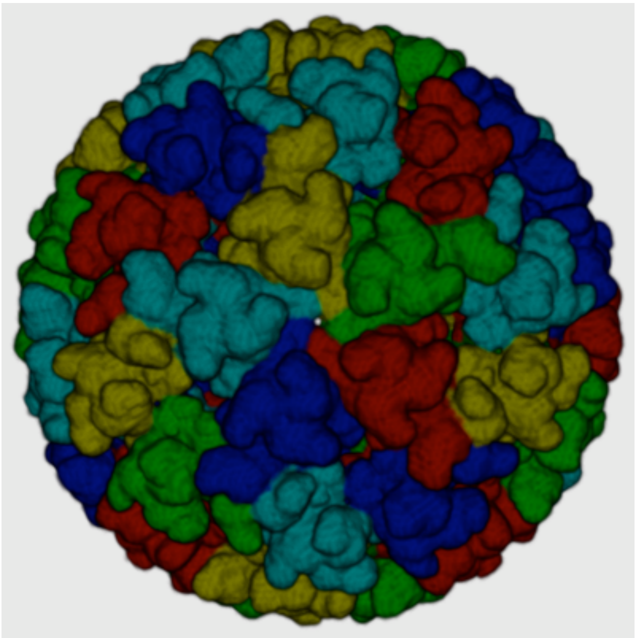

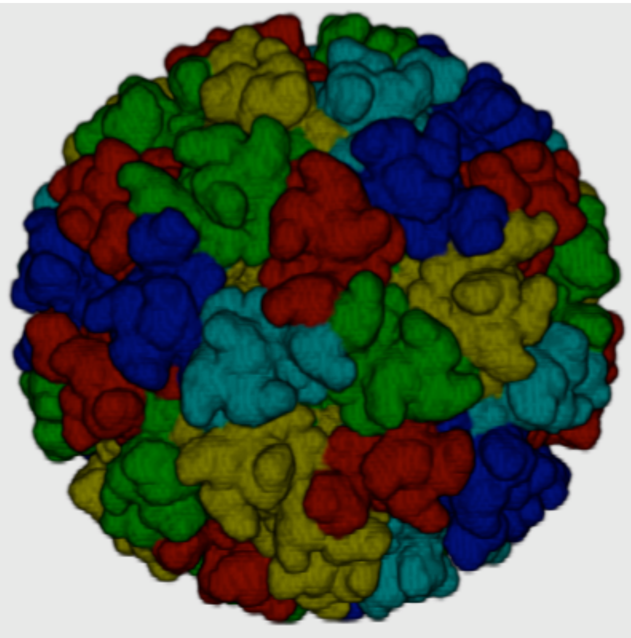

segmented capsid layer

segmented asymmetric subunits (five-fold & three-fold)

Results: Synthetic Map

PDB ID = 1HB9, San Martin et al 2001

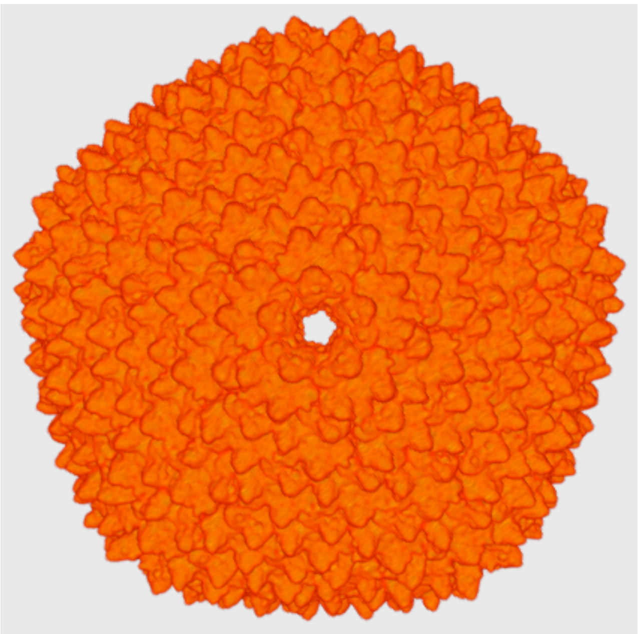

synthetic capsid layer

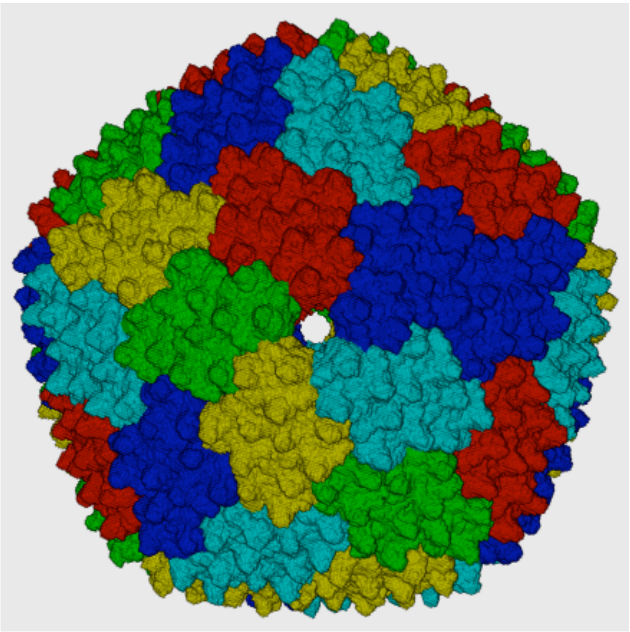

asymmetric subunits (our method)

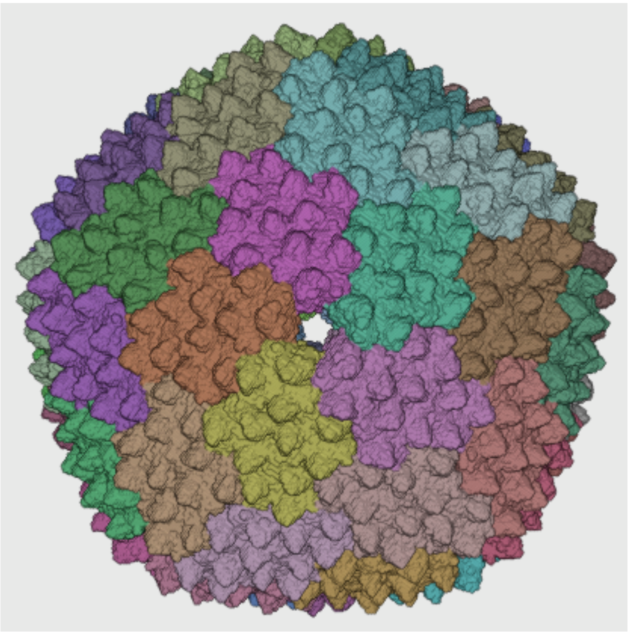

true segmentation

Results: Synthetic Map

PDB ID = 1HB9, San Martin et al 2001

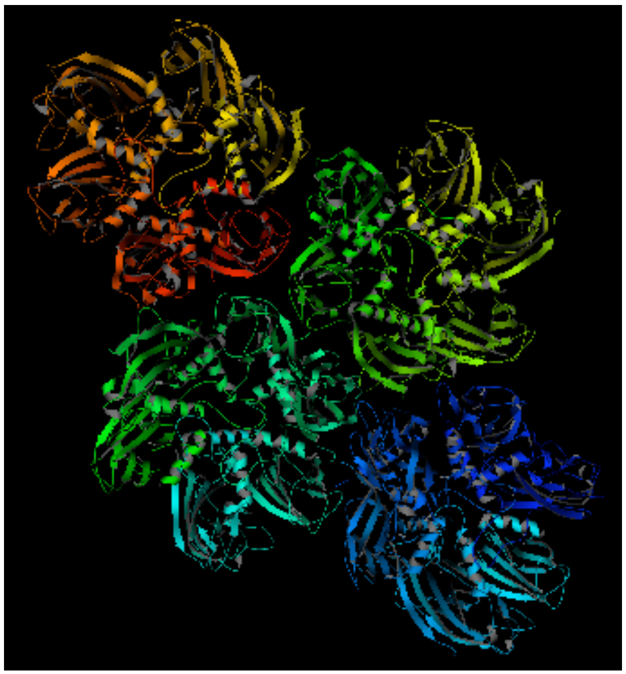

crystal structure of subunit

blurred map

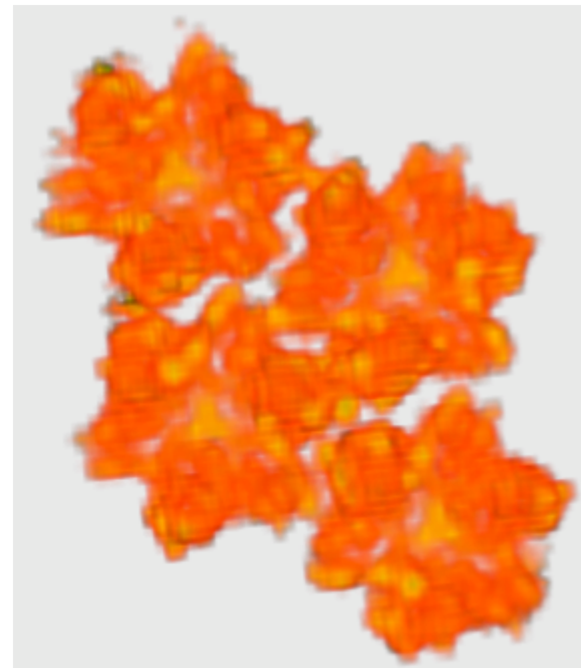

one subunit of our result

Gradient Vector Diffusion (GVD)

- Partial Differential Equation (Xu and Prince, 1998)

$$\begin{cases} \dfrac{\partial u}{\partial t} = \mu \nabla^2 u - (u - f_x)(f_x^2 + f_y^2) \\ \dfrac{\partial v}{\partial t} = \mu \nabla^2 v - (v - f_y)(f_x^2 + f_y^2) \end{cases}$$

where (u(t), v(t)) stands for the evolving vector field;

μ is a constant;

f is the original image to be diffused;

(f_x, f_y) = (u(0), v(0)).

- Polar-representation version of GVD (Yu and Bajaj, ICPR02)

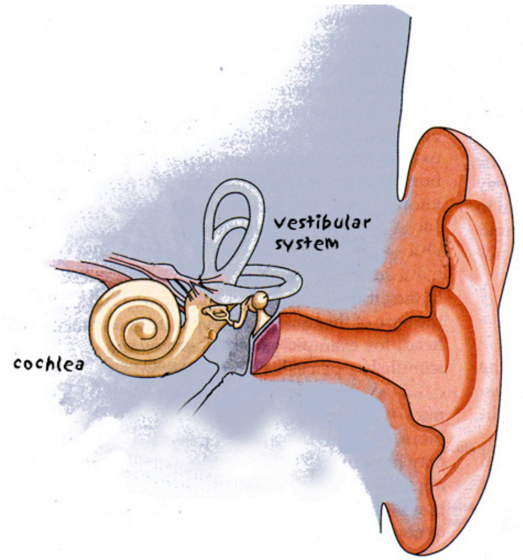

medical and biological importance of hearing

- 1 child in 1000 is born deaf
- 30 million Americans suffer from severe hearing problems (~10% of population)
- large bandwidth — 20 - 20,000 Hz (up to 100,000 Hz)
- high fidelity — 0.1% discrimination (1 Hz @ 1000 Hz)
- high sensitivity — responds to sound-driven vibration of 3Å
- outstanding amplification — -> otoacoustic emissions
- high speed of detection — 10 μs -> direct mechanical transduction
- high dynamic range — 10^6 / 0-120 dB -> adaptation

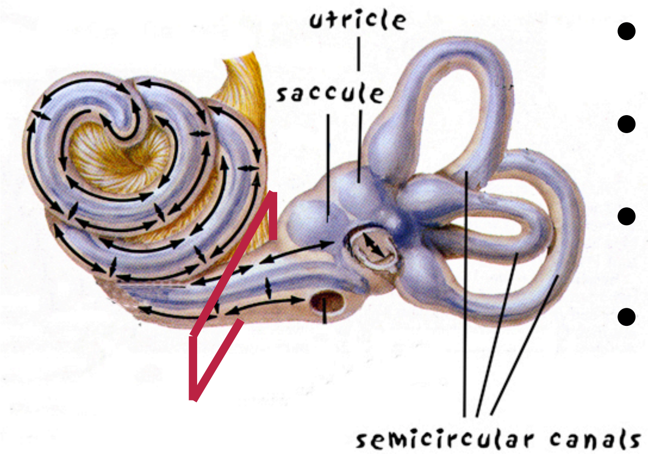

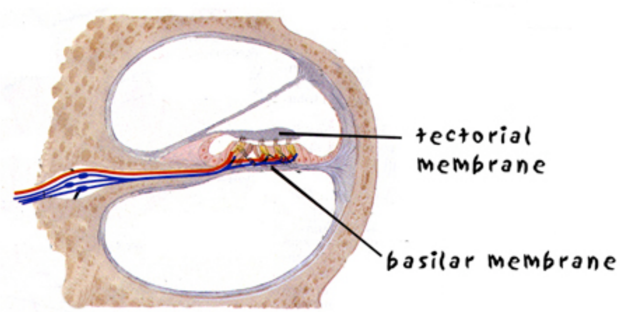

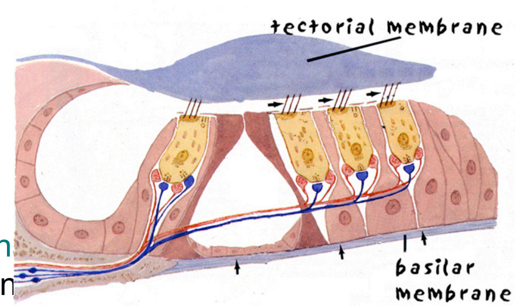

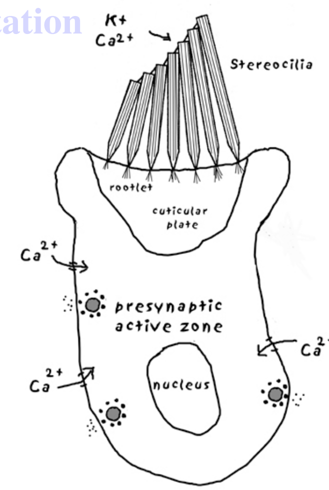

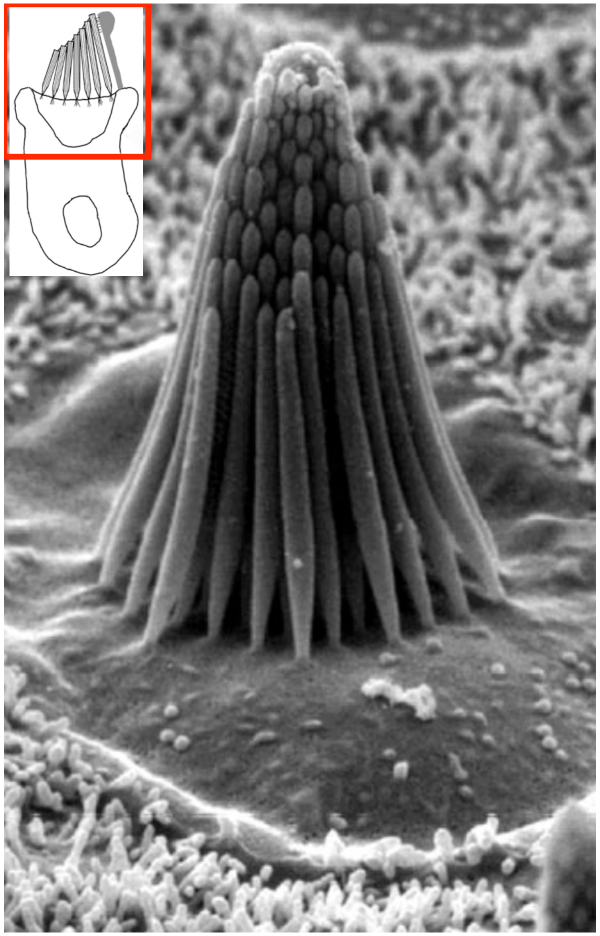

1977-1987 Hudspeth & Corey

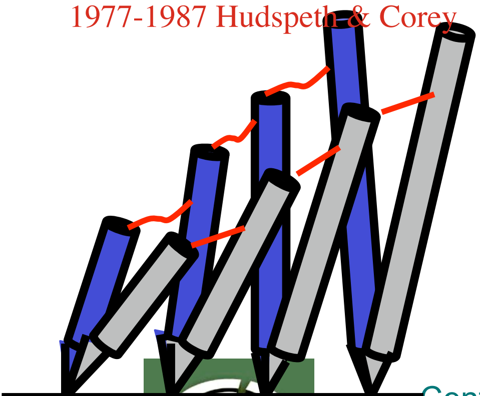

hair bundle - hearing organelle of the hair cell

- direct mechanotransduction	1-2 channels/stereocilium
- adaptation machinery	via non-conventional myosin 1c
- amplification	spontaneous bundle oscillation, driven by myosin-motor proteins

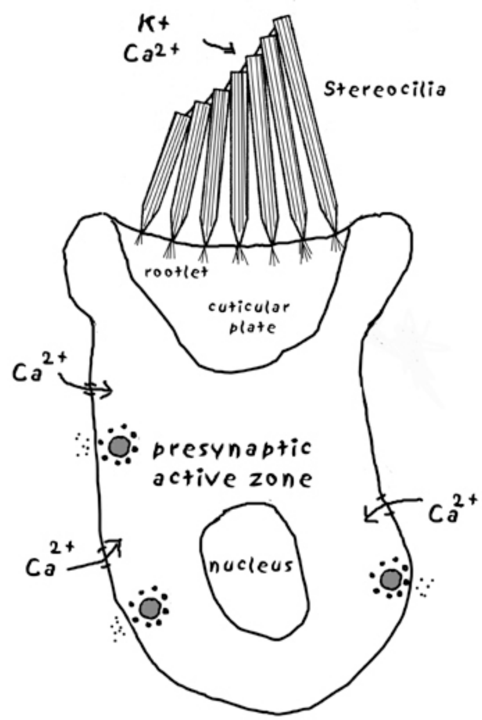

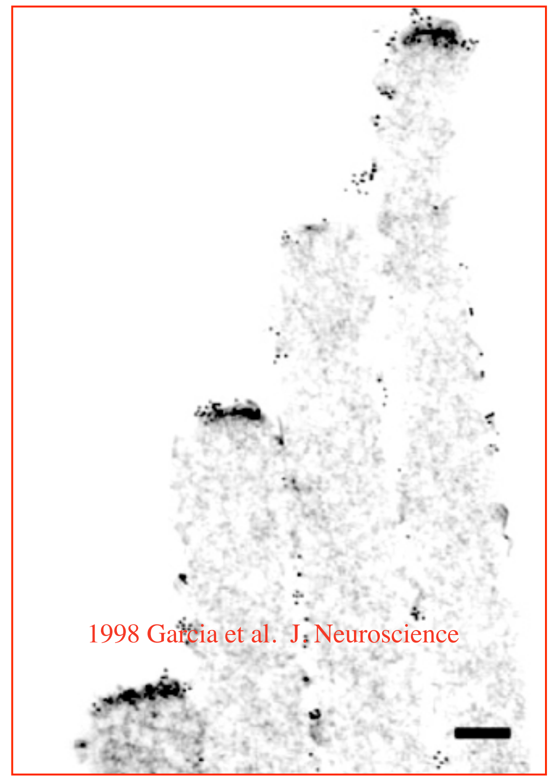

1998 Garcia et al. J. Neuroscience

transduction & adaptation

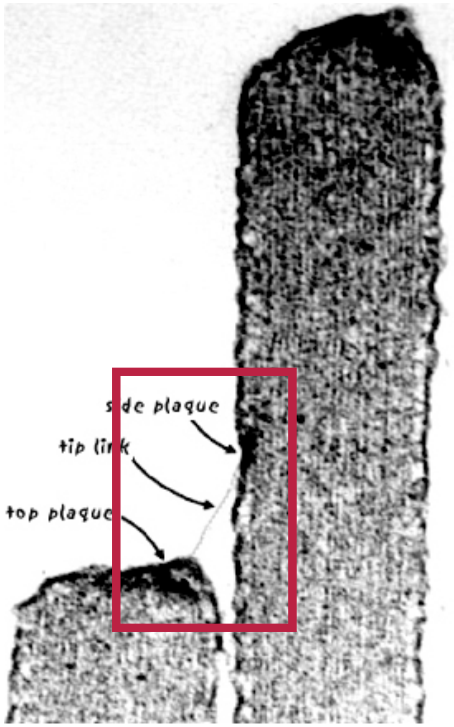

- mechanical stretching of tip links opens mechanosensitive channel

- membrane depolarisation by K^+, fast channel reclosure by Ca^{2+}

- slipping of adaptation machinery by conformational changes of myosin motor domain upon Ca^{2+} binding to calmodulin/IQ domain

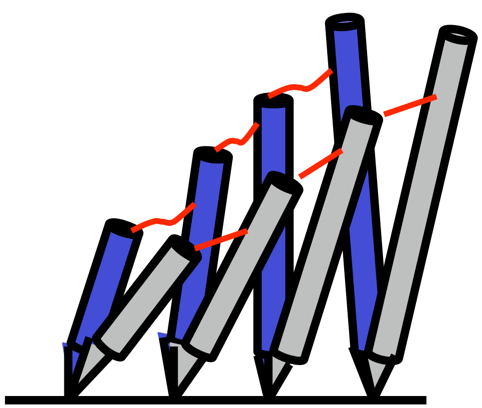

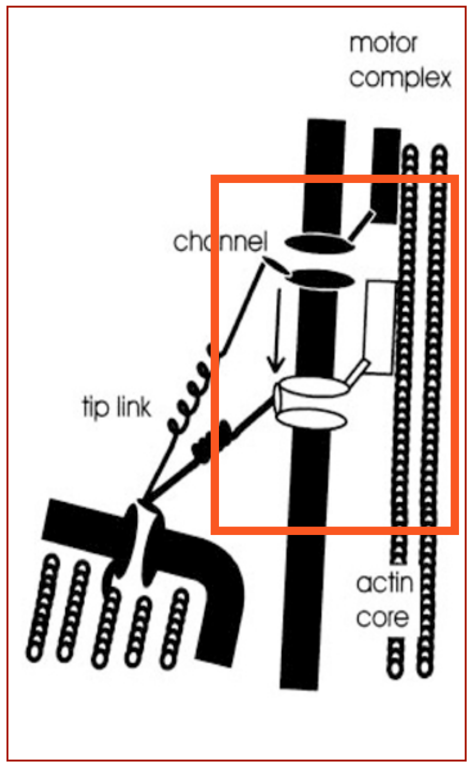

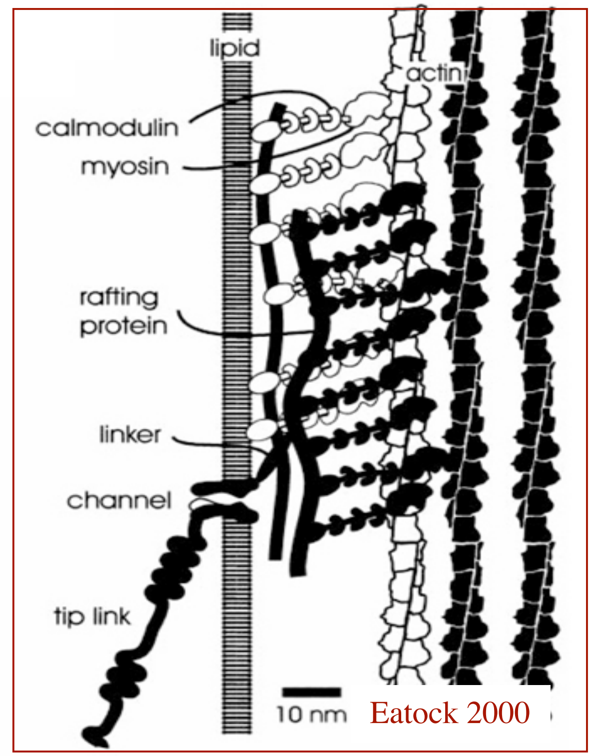

Center for Comp
Institute of Comp
Department of Computer Sciences
Uni

Detergent Extraction
&
PLT dehydration

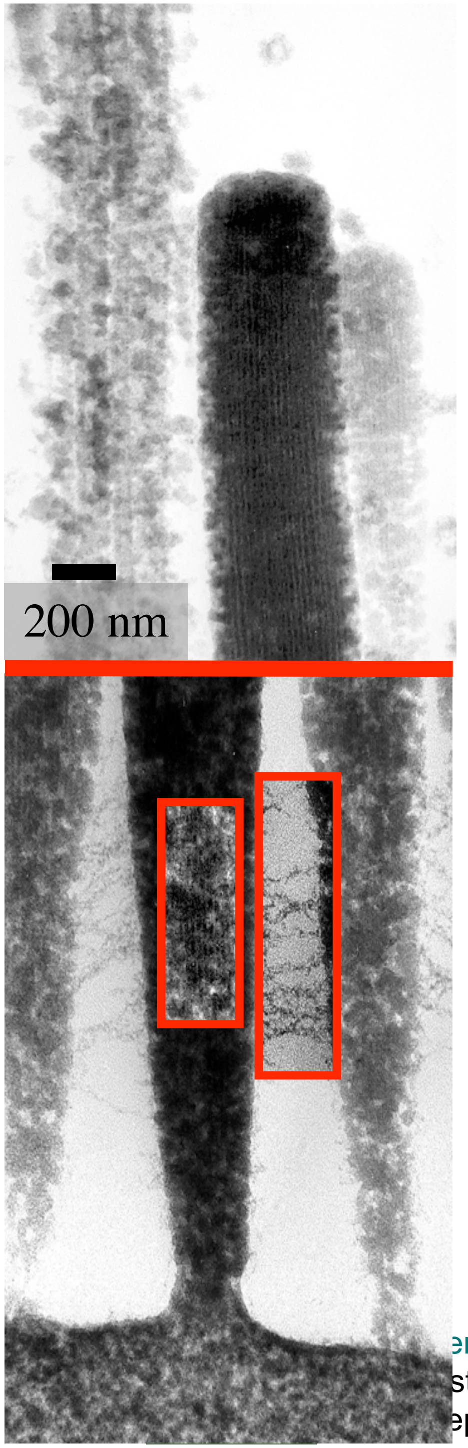

- membranes partially dissolve
- raft-like structures remain
- actin filaments are well preserved
- extracellular links remain intact

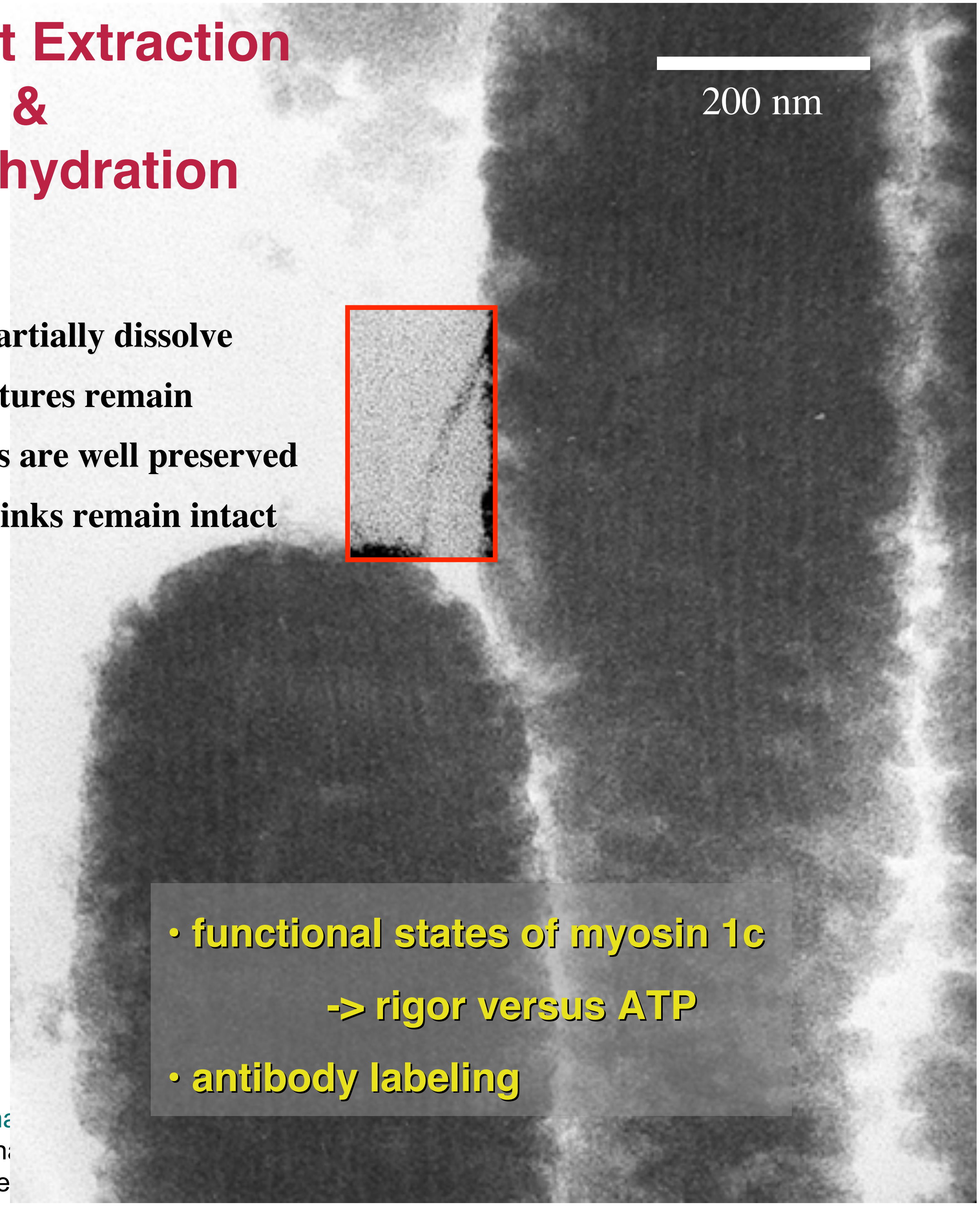

• functional states of myosin 1c

-> rigor versus ATP

• antibody labeling

Imaging of a cell organelle

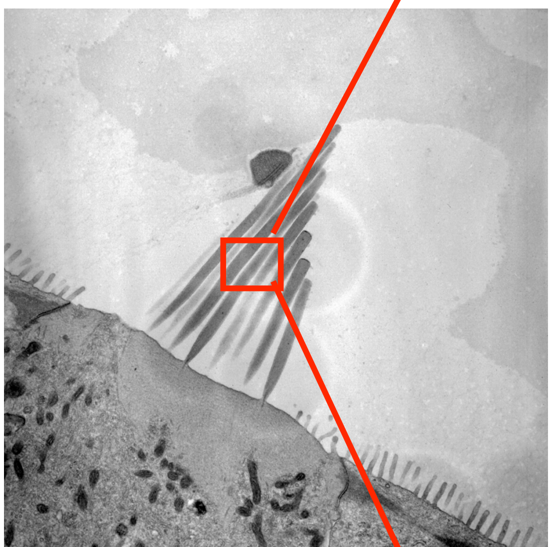

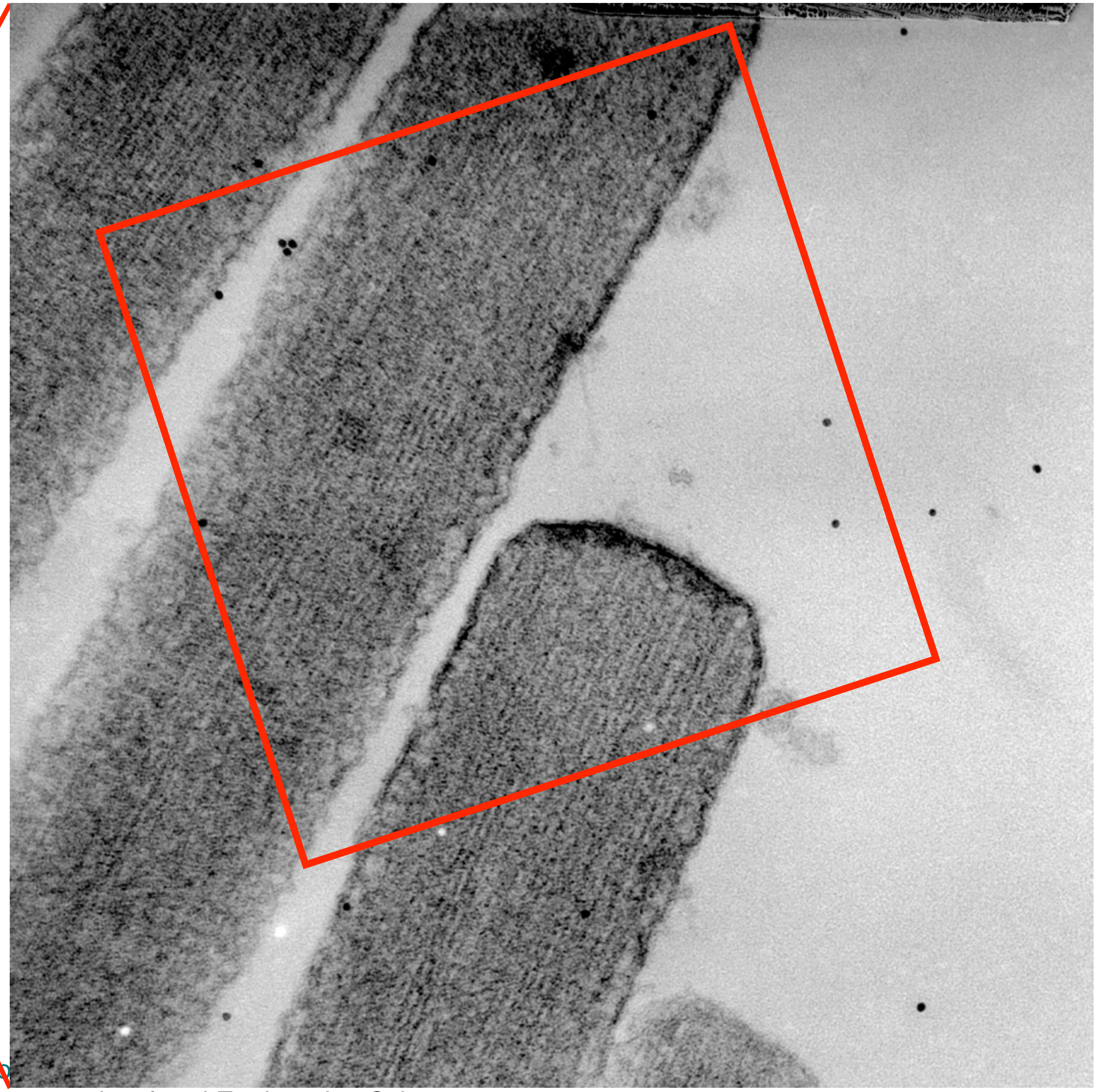

structural organization of the adaptation machinery

- electronic "dissection" of the motor complex -

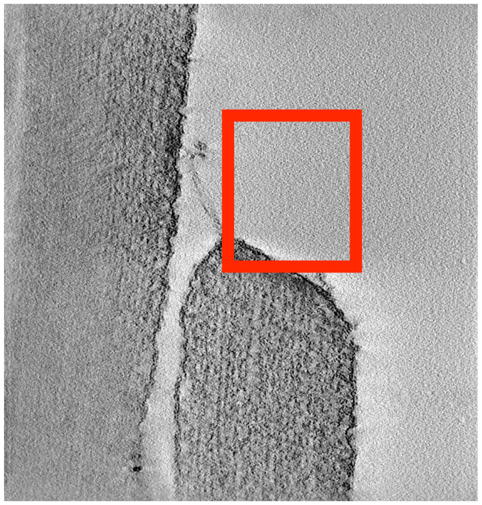

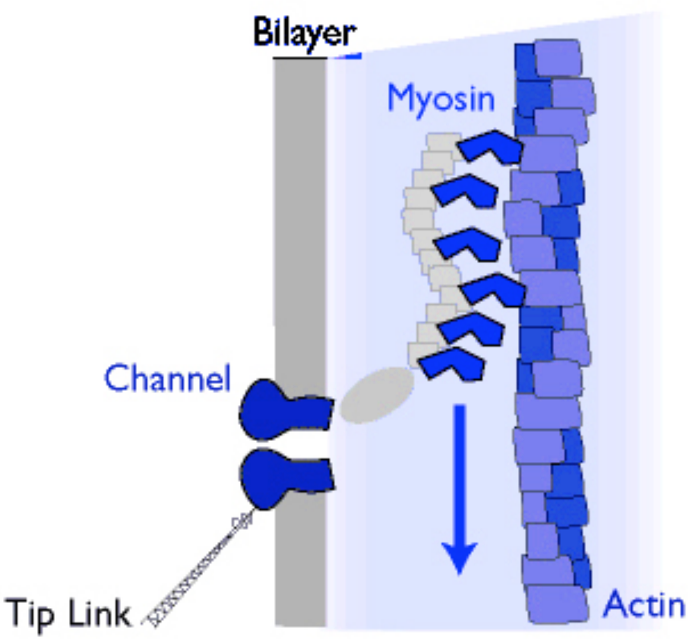

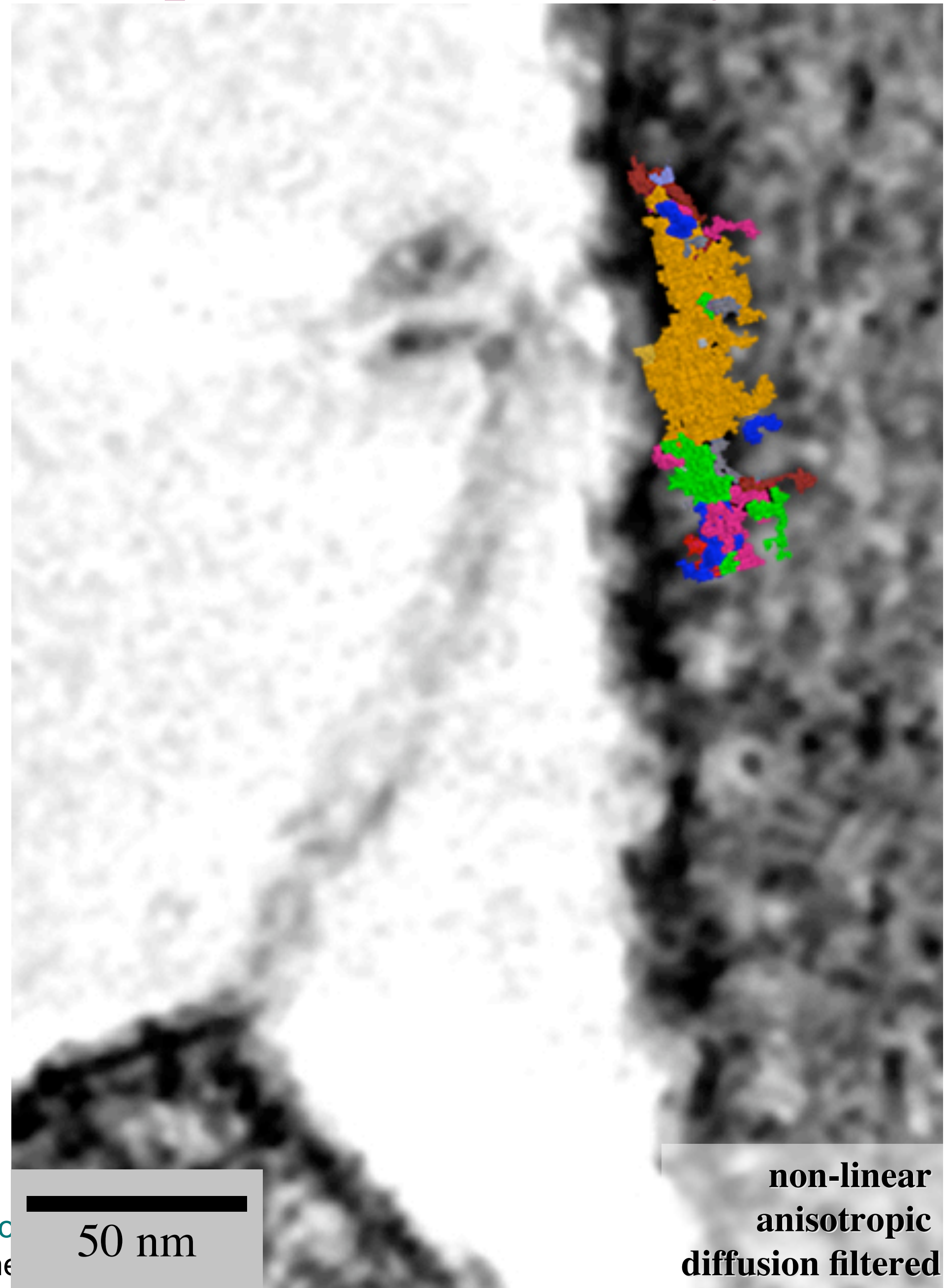

Side Plaque

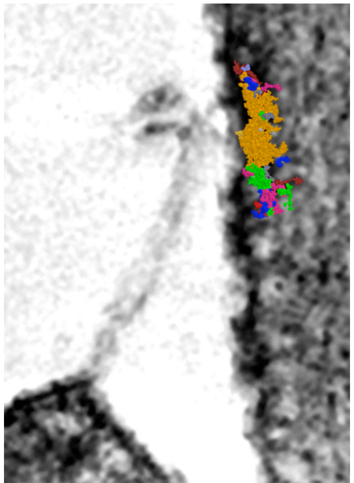

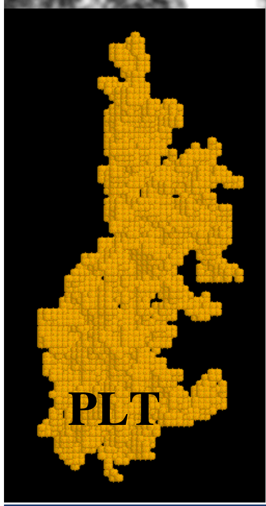

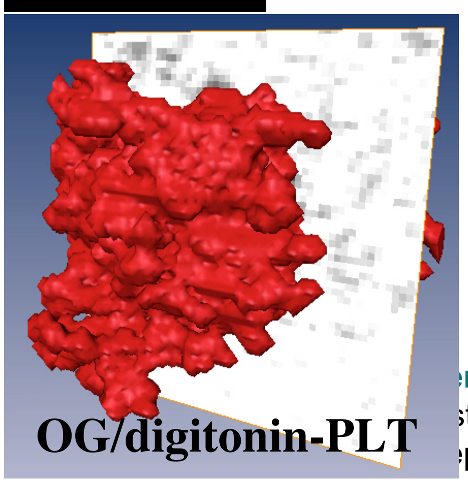

20 nm

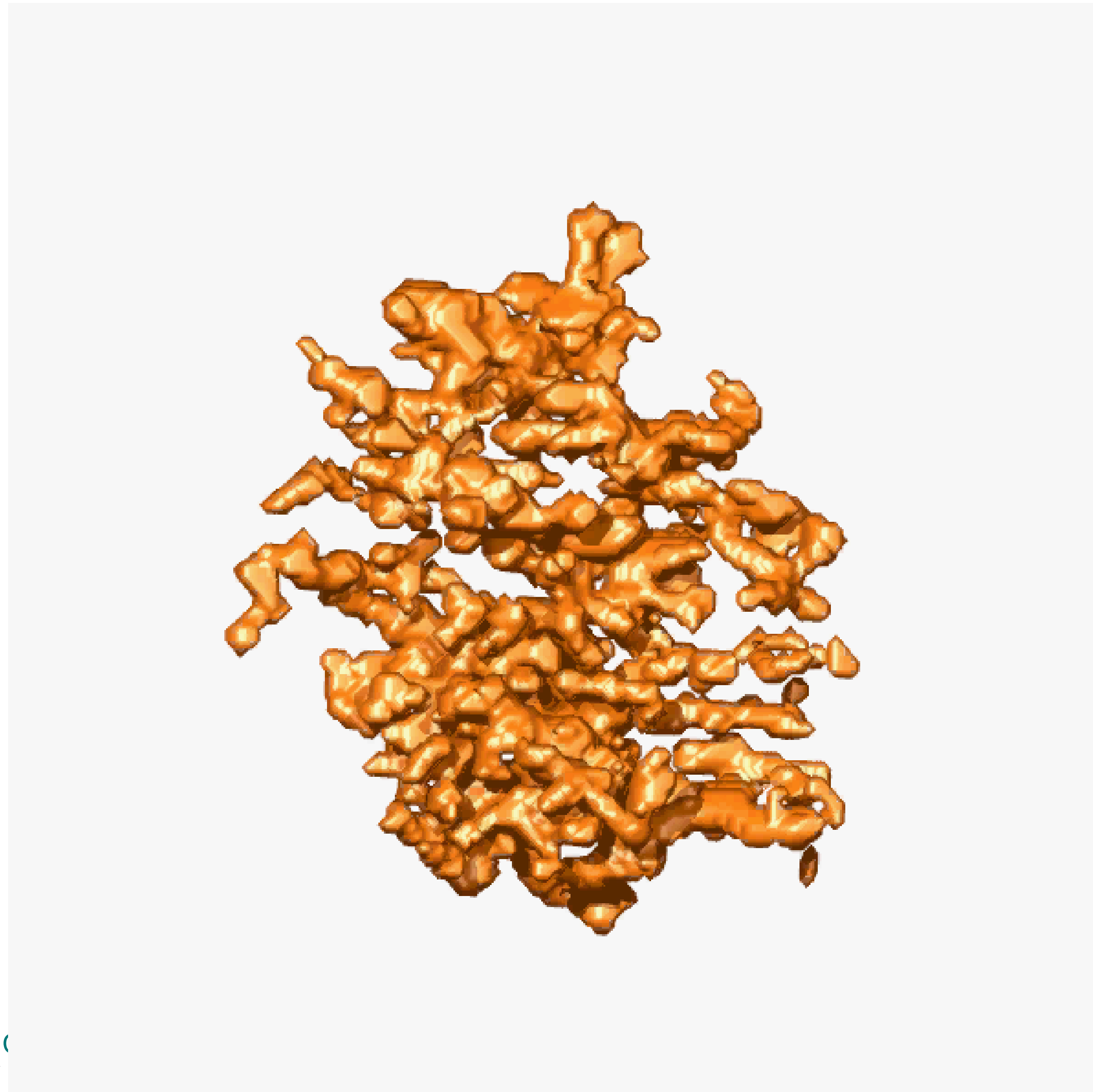

2nd TIPLINK

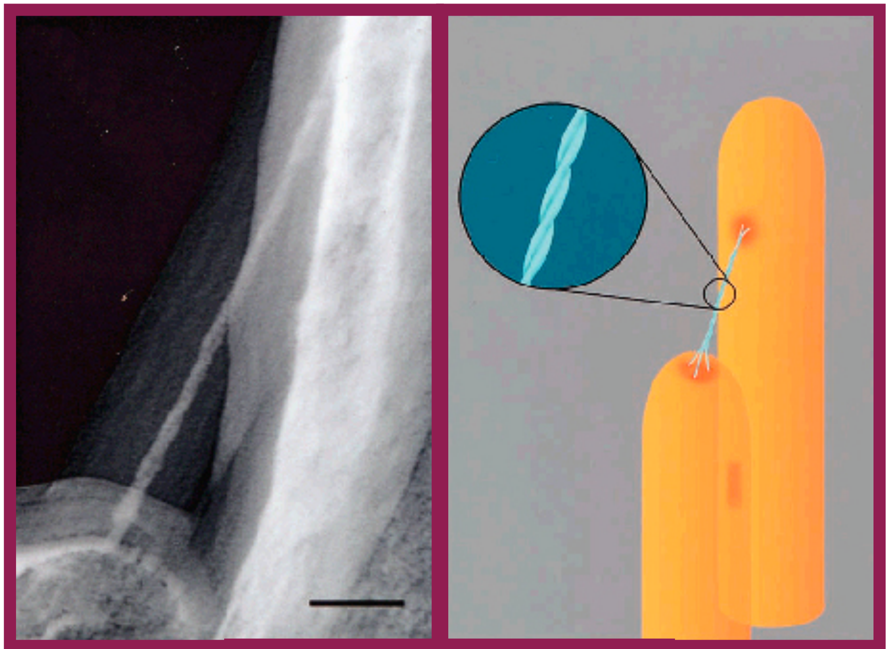

Kachar et al 2000 PNAS

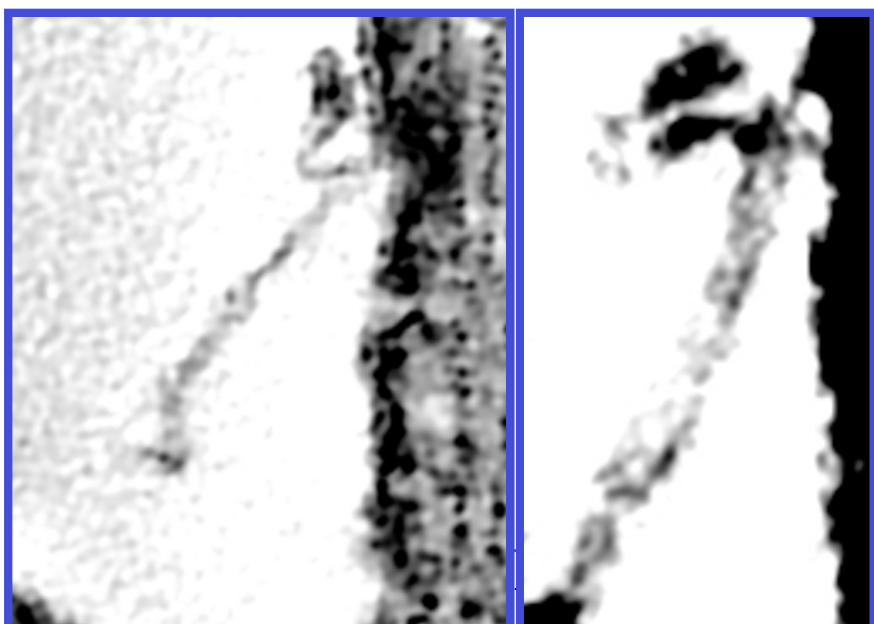

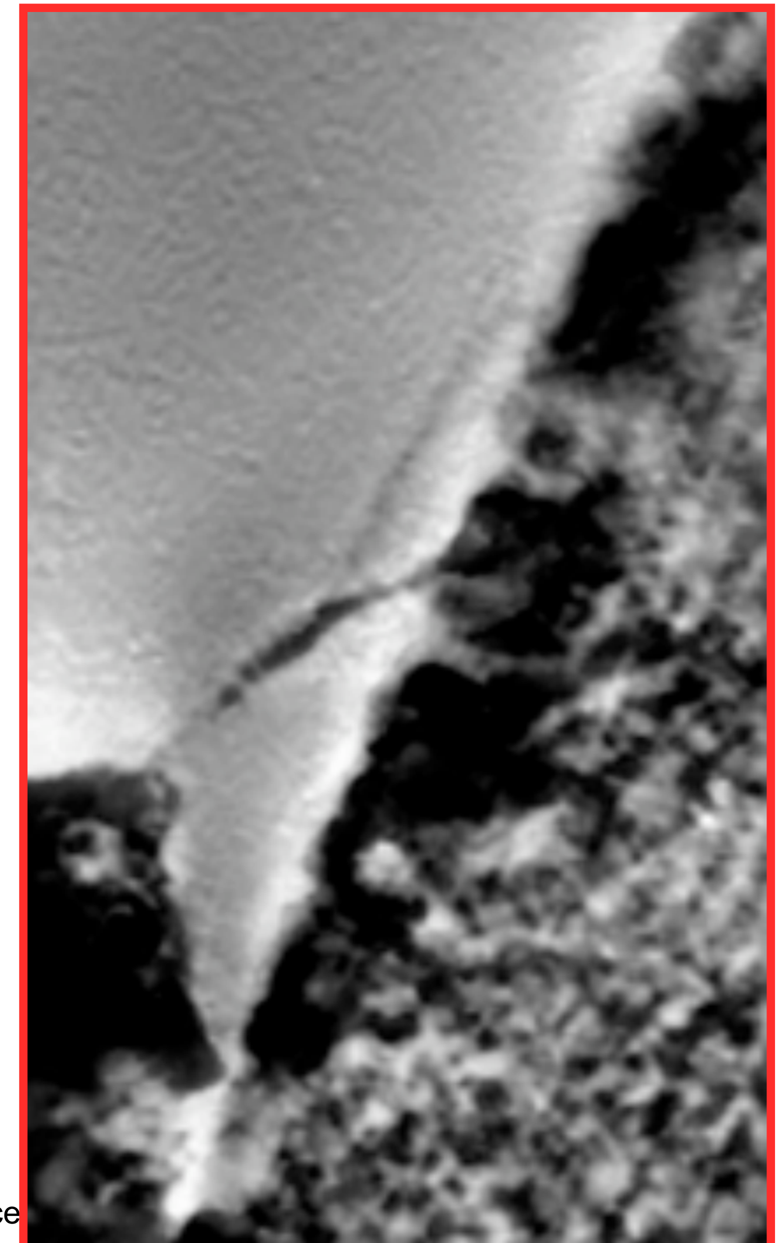

TipLink-Cilia

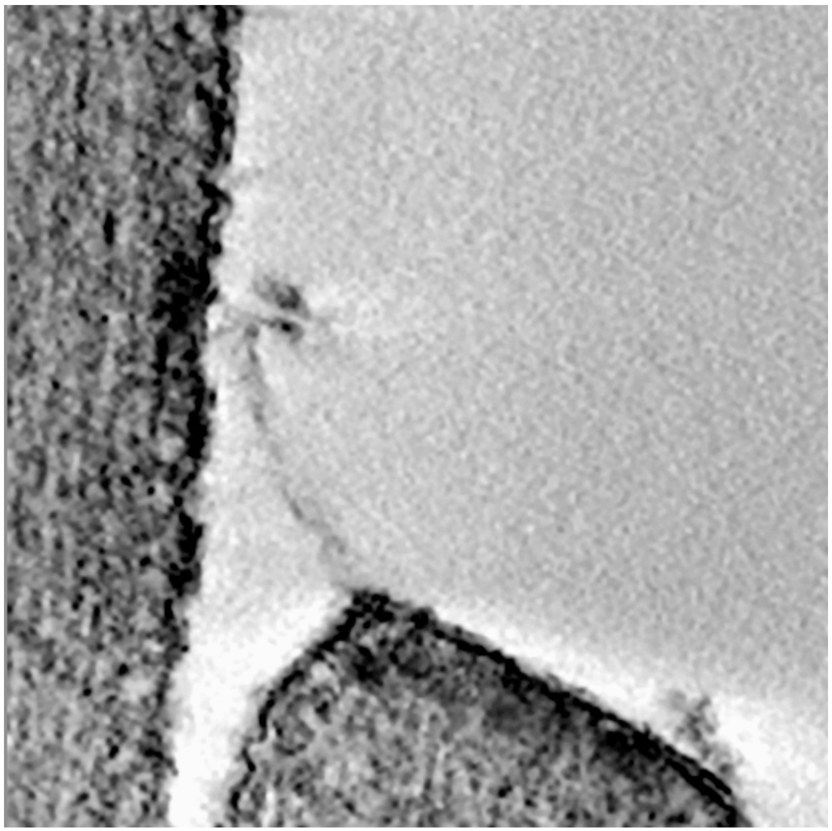

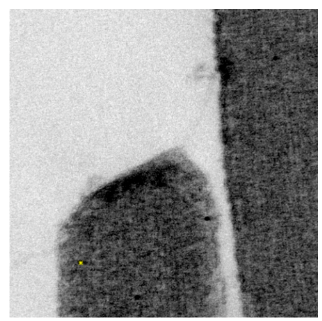

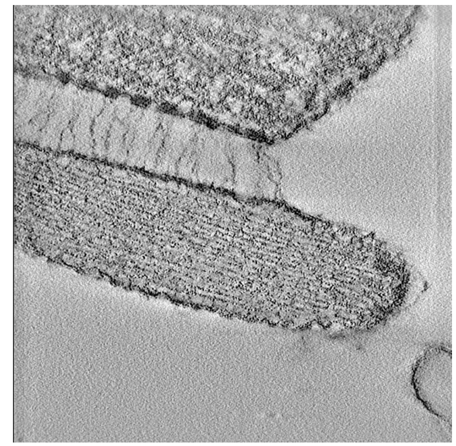

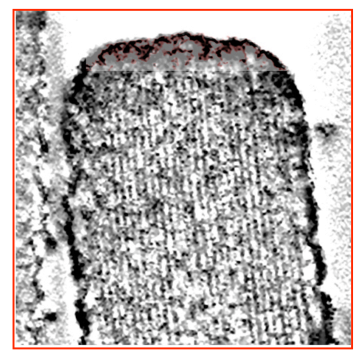

Compute Critical Points Using GVD

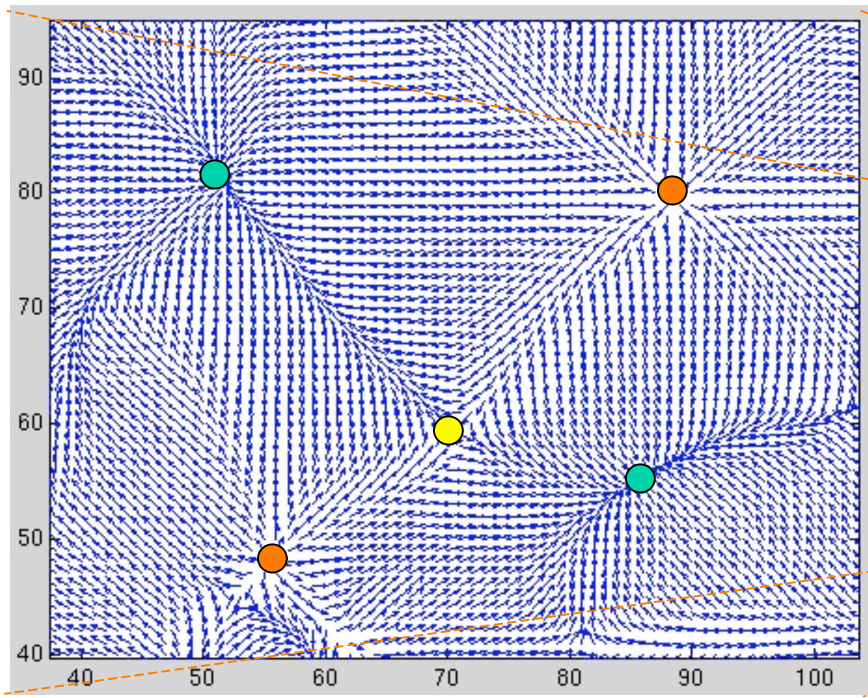

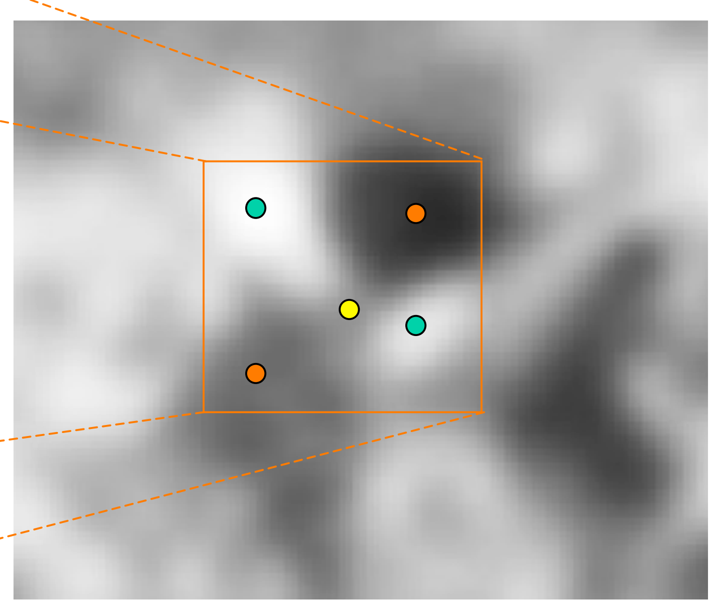

●: minimum ●: maximum ●: saddle

How GVD Helps Image Segmentation ?

- Fast Marching Method
  - Initial seed points
  - Stopping criterion

- Use GVD to locate seed points
  - Compute min/max critical points using GVD (discard saddle critical points)
  - All such critical points are used as seeds
  - Advantages: automatic, close to centers of homogenous regions, robust to noise due to vector diffusion.

Stopping Criteria Using Multiple-Contour

- Multiple-Contour
  - Group the critical points (for example, two groups as follows: max. critical points → feature & min. critical points → background)
  - Each seed initializes one contour, coupled with its group's I.D.
  - Contours march simultaneously. Contours with same I.D. are merged while contours with different I.D. stop on their common boundaries

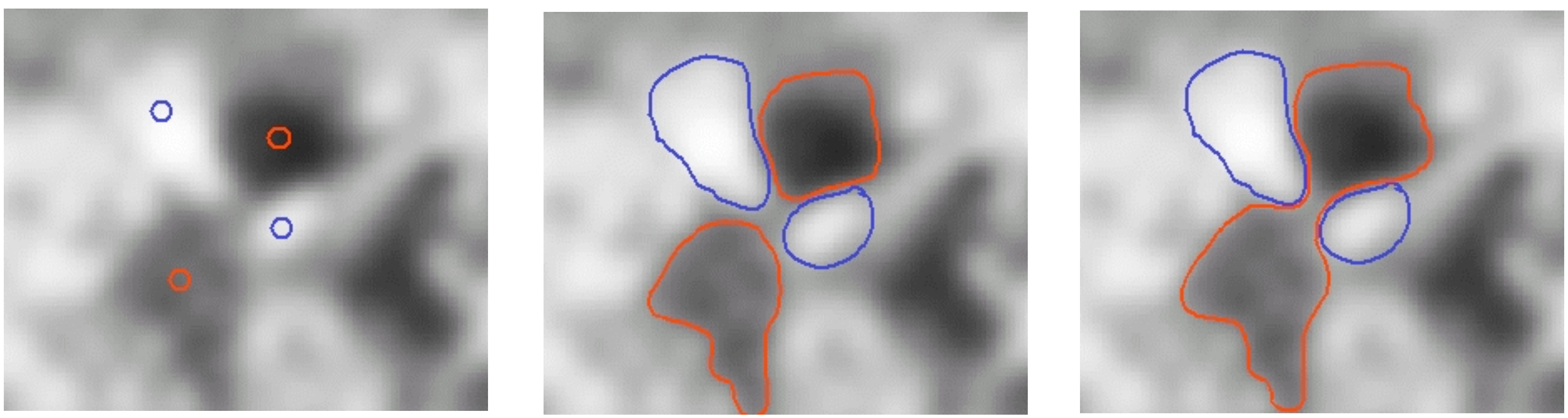

Segmentation of TipLink (B206a)

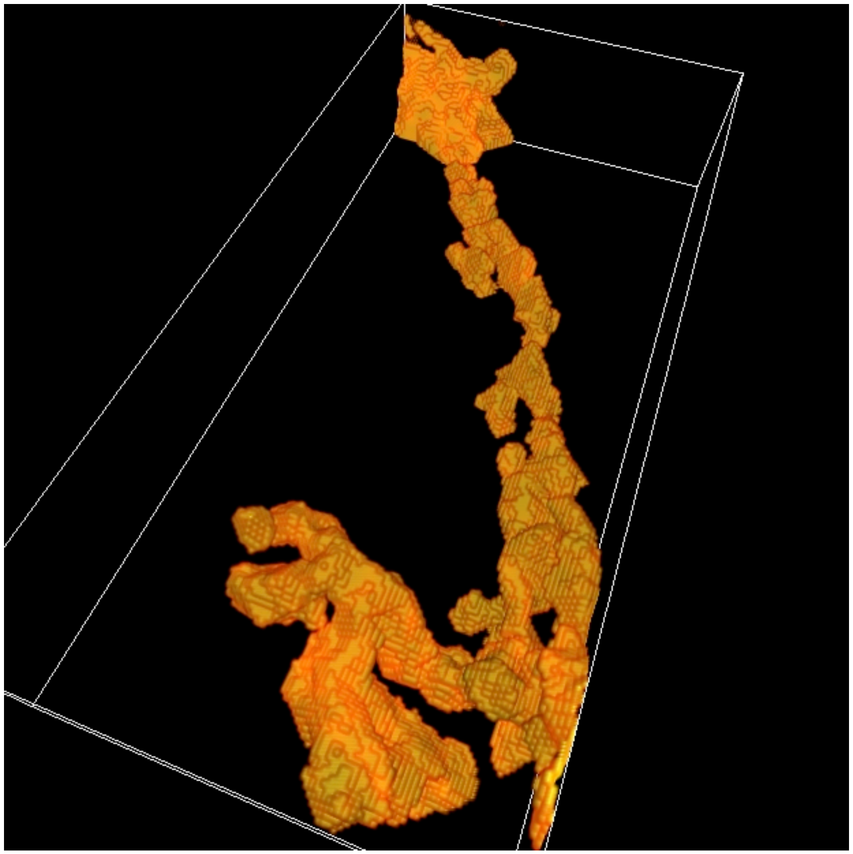

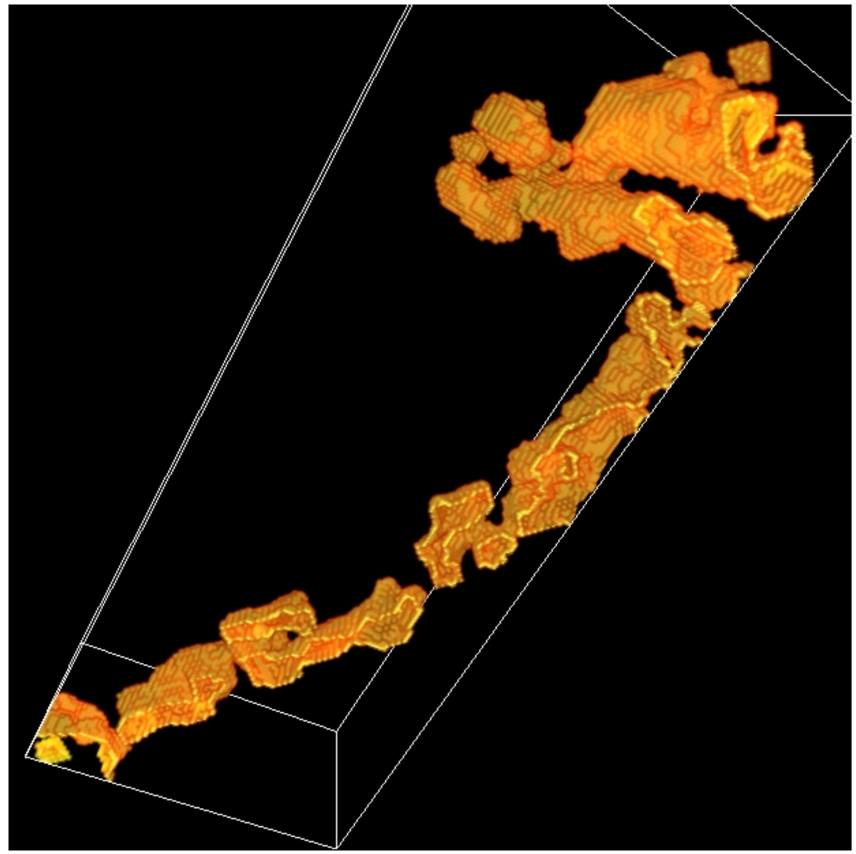

How GVD Helps Image Skeletonization ?

- Use GVD to locate critical points
  - Include minimum/maximum/saddle critical points
- Start from saddle points; trace integral lines along the diffused gradient vector field $\Longrightarrow$ Morse graph
- Prune the Morse graph for more meaningful skeletons
- Advantages:
  - Robust to noise due to vector diffusion.
  - Critical points are on the “skeletons” of features even for “flat” regions.

Skeletons of ActinBundle (B280a)

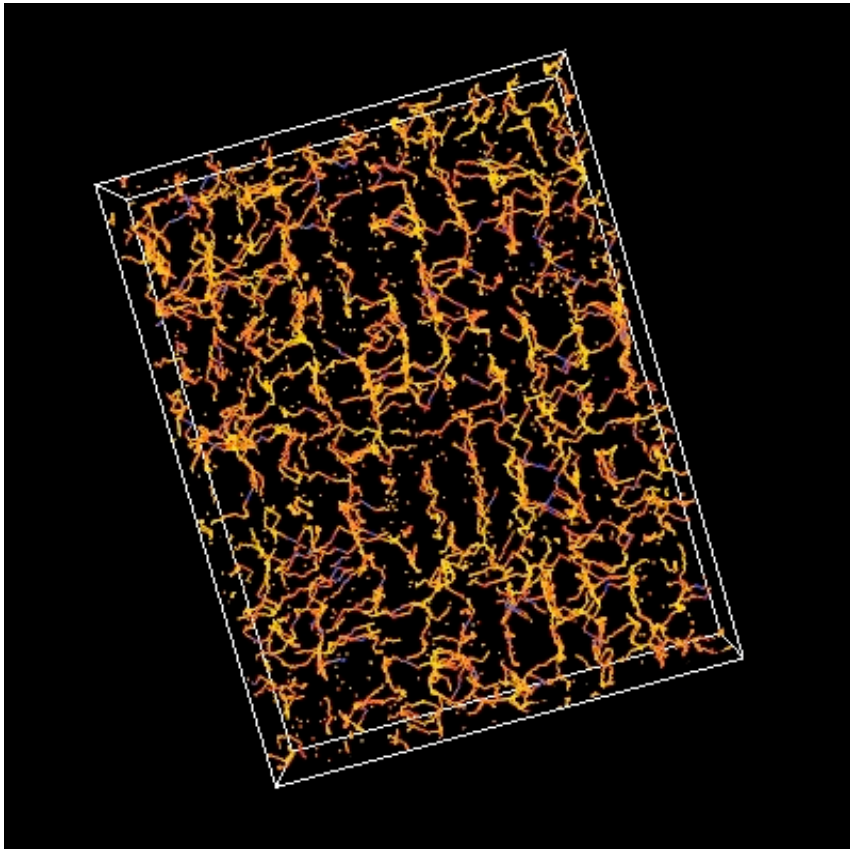

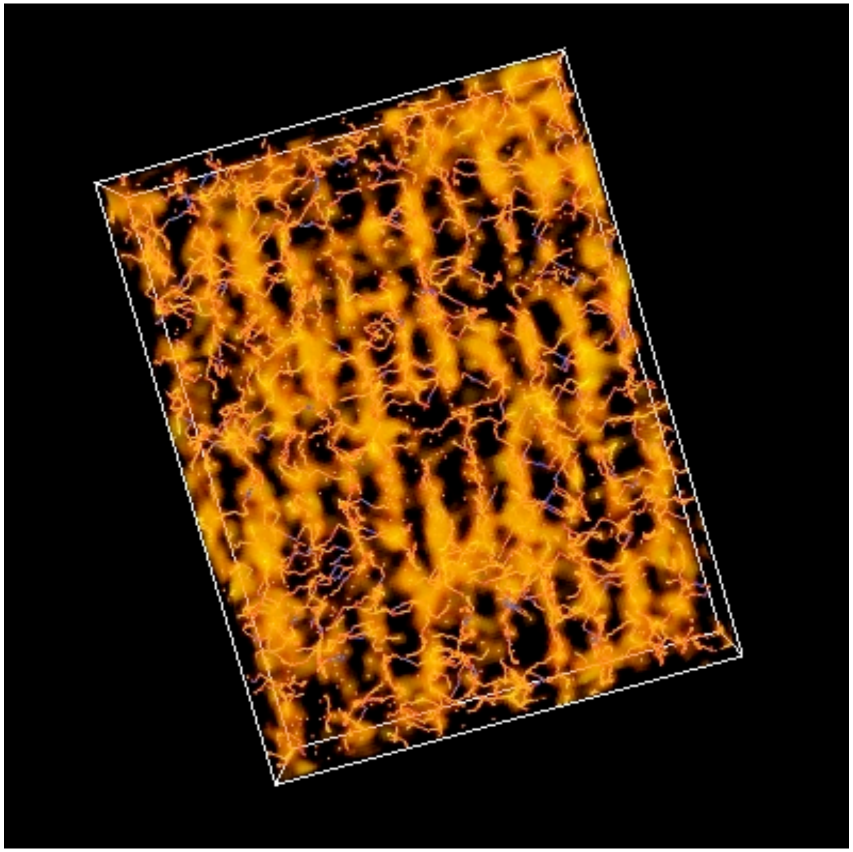

Reading

1. Z. Yu, C. Bajaj **Computational Approaches for Automatic Structural Analysis of Large Bio-molecular Complexes** *IEEE/ACM Transactions on Computational Biology and Bioinformatics, June 2007*
2. C. Bajaj, G. Xu, Q. Zhang **Bio-Molecule Surfaces Construction Via a Higher-Order Level Set Method** *Proceedings of the 14th CAD/CG International Conference, 2007, Beijing, China*
3. G. Xu, Q. Pan, C. Bajaj **Discrete Surface Modelling Using Partial Differential Equations** *Computer Aided Geometric Design, Volume 23/2, pp 125-145, 2006.*
4. Z. Yu, C. Bajaj **Automatic Ultrastructure Segmentation of Reconstructed CryoEM Maps of Icosahedral Viruses** *IEEE Transactions on Image Processing: Special Issue on Molecular and Cellular Bioimaging, 2005 Sep;14(9):1324-37*
5. C. Bajaj, Z. Yu, M. Auer **Volumetric Feature Extraction and Visualization of Tomographic Molecular Imaging** *Journal of Structural Biology, Volume 144, Issues 1-2, October 2003, Pages 132-143*
6. Z. Yu, C. Bajaj **A Fast and Adaptive Algorithm for Image Contrast Enhancement** *Proceedings of 2004 IEEE International Conference on Image Processing (ICIP'04), Volume 2, Oct. 24-27 2004, Pages 1001-1004, Singapore.*
7. Z. Yu, C. Bajaj **A Segmentation-Free Approach for Skeletonization of Gray-Scale Images via Anisotropic Vector Diffusion** *Proceedings of 2004 IEEE International Conference on Computer Vision and Pattern Recognition (CVPR'04), Volume 1, Pages 415-420, Washington, DC.*
8. C. Bajaj, J. Chen, R. Holt, A. Netravali **Energy Formulations of A-Splines** *Computer Aided Geometric Design, 16:1(1999), 39-59.*